



8-1995

## Ultraviolet Spectrometric Characterization of Metal Decontamination

Vivekanand Sistla  
*University of Tennessee, Knoxville*

Follow this and additional works at: [https://trace.tennessee.edu/utk\\_gradthes](https://trace.tennessee.edu/utk_gradthes)

---

### Recommended Citation

Sistla, Vivekanand, "Ultraviolet Spectrometric Characterization of Metal Decontamination. " Master's Thesis, University of Tennessee, 1995.  
[https://trace.tennessee.edu/utk\\_gradthes/6232](https://trace.tennessee.edu/utk_gradthes/6232)

This Thesis is brought to you for free and open access by the Graduate School at TRACE: Tennessee Research and Creative Exchange. It has been accepted for inclusion in Masters Theses by an authorized administrator of TRACE: Tennessee Research and Creative Exchange. For more information, please contact [trace@utk.edu](mailto:trace@utk.edu).

To the Graduate Council:

I am submitting herewith a thesis written by Vivekanand Sistla entitled "Ultraviolet Spectrometric Characterization of Metal Decontamination." I have examined the final electronic copy of this thesis for form and content and recommend that it be accepted in partial fulfillment of the requirements for the degree of Master of Science, with a major in Chemical Engineering.

M. G. Hansen, Major Professor

We have read this thesis and recommend its acceptance:

Tse-Wei Wang, Robert Counce

Accepted for the Council:

Carolyn R. Hodges

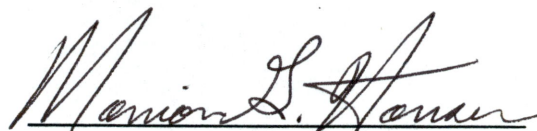
Vice Provost and Dean of the Graduate School

(Original signatures are on file with official student records.)



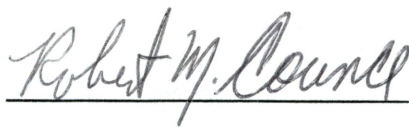
To the Graduate Council :

I am submitting herewith a thesis written by Vivekanand Sistla entitled "Ultraviolet Spectrometric Characterization of Metal Decontamination". I have examined the final copy of this thesis for form and content and recommend that it be accepted in partial fulfillment of the requirements for the degree of Master of Science, with a major in Chemical Engineering.



M. G. Hansen, Major Professor

We have read this thesis  
and recommend its acceptance



Accepted for the Council



Associate Vice Chancellor and  
Dean of The Graduate School

# ULTRAVIOLET SPECTROMETRIC CHARACTERIZATION OF METAL DECONTAMINATION

A Thesis

Presented for the

Master of Science

Degree

The University of Tennessee, Knoxville

Vivekanand Sistla

August 1995

This thesis is dedicated to my mother

Janaki

## ACKNOWLEDGEMENTS

I would like to thank Dr. Marion Hansen, my major professor, for his guidance, and for his patience during the course of this project. I am thankful to Dr. Tse-Wei Wang who introduced me to the concepts of multivariate data analysis, and to Dr. Robert Counce for several useful suggestions. The staff at the Oak Ridge National Laboratories was extremely cooperative and helped me with various experiments. I would especially like to thank Ms. Lynn Glover, Dr. G. L. Powell and Dr. Tye Barber for their assistance. My colleagues Chris Stafford and Rodney Mackereth provided technical support and made this project more fun to work on. Thanks are due to fellow graduate students Atul Khettry, Raju Batra, and Srini Vedula for their encouragement and advice. The financial support provided by the Environmental Protection Agency is acknowledged. Finally, a big thank you to my family for their unflinching support, without which this work would not have been possible.

## ABSTRACT

The viability of an ultraviolet fiber optic method for quantifying contamination levels on metal substrates was demonstrated. Contaminated metal samples obtained from industrial processing operations were cleaned with alternative solvents being used to replace chlorofluorocarbons, which are in the process of being phased out. Cleaned samples with varying amounts of oils remaining on them were analyzed for residual amounts using four testing methods: X-ray spectroscopy, infrared spectroscopy, ultraviolet spectroscopy, and gravimetric analysis.

Multivariate data analysis techniques were used to prepare a model using ultraviolet and infrared data. Both principal component regression (PCR) and partial least squares (PLS) methods were used in the analysis of the data. A one-factor model was found to be adequate for the infrared data. Interpretation of the results using different types of cross validation showed that two factors were required for the ultraviolet model. Cleanliness levels were also determined using electron scanning for chemical analysis (ESCA) and gravimetric methods. The results from all four methods were expressed in terms of amount of contamination in milligrams per unit area. The values obtained were compared against actual contamination data, and the sum of squares of errors was calculated. The predicted residual sum of squares of error for an equal number of comparison points for IR, UV, ESCA, and gravimetry were 0.20, 0.84, 1.39, and 2.54 (mg. /ft.<sup>2</sup>)<sup>2</sup> respectively. The predictive ability of each method was

related to its cost and ease of use. The ultraviolet instrumentation tested in this study ranked second in predictive ability and second in cost, making it a viable option for cleanliness testing purposes.



# TABLE OF CONTENTS

Chapter	Page
<b>1. INTRODUCTION</b> .....	1
1.1 Problem Statement .....	1
<b>2. BACKGROUND</b> .....	4
2.1 Ozone Layer Depletion .....	4
2.2 Alternate Cleaning Techniques .....	6
2.2.1 Alternate Cleaning Chemistries .....	7
2.2.2 Alternate Cleaning Technologies .....	8
2.3 Spectroscopic Methods .....	13
2.3.1 Electron Scanning for Chemical Analysis (ESCA or XPS). .....	13
2.3.2 Infrared Spectroscopy .....	17
2.3.3 Ultraviolet Spectroscopy .....	18
2.3.4 Sampling Methods .....	18
2.4 Multivariate Data Analysis .....	20
2.4.1 Least Squares Methods.....	21
2.4.2 Principal Component Regression .....	23
2.4.3 Partial Least Squares .....	26
2.4.4 Evaluation of Regression Results .....	28
<b>3. LITERATURE REVIEW</b> .....	30
3.1 Testing Surfaces for Cleanliness .....	30
3.2 Review of Spectroscopic Methods .....	40

3.2.1 XPS and Surface Analysis .....	40
3.2.2 Applications of Infrared Spectroscopy .....	43
3.2.3 Ultraviolet Region .....	47
<b>4. EXPERIMENTAL METHODS .....</b>	<b>51</b>
4.1 Decontamination of Metal Parts .....	51
4.2 Cleanliness Testing Using ESCA .....	54
4.3 Cleanliness Testing Using Infrared .....	55
4.4 Cleanliness Testing using Ultraviolet .....	57
4.5 Cleanliness Testing by Gravimetric Analysis .....	59
<b>5. RESULTS AND DISCUSSION .....</b>	<b>63</b>
5.1 Results from ESCA .....	63
5.2 Results from Infrared Spectroscopy .....	72
5.3 Results from Ultraviolet Fiber Optic Spectroscopy .....	76
5.4 Results from Gravimetric Testing .....	79
5.5 Correlation of Results from Various Testing Methods .....	82
5.5.1 Infrared vs. Ultraviolet .....	82
5.5.2 Ultraviolet vs. Gravimetric .....	93
5.5.3 Ultraviolet vs. ESCA .....	97
5.5.4 Comparison of Techniques .....	98
<b>6. CONCLUSIONS AND FUTURE WORK .....</b>	<b>105</b>
6.1 Conclusions .....	105
6.2 Future Work .....	106



BIBLIOGRAPHY .....	108
--------------------	-----

VITA .....	117
------------	-----

## LIST OF FIGURES

Figure	Page
2.1 A typical cleaning and recycling closed loop for aqueous and semi-aqueous formulations .....	11
2.2 Schematic showing the basic components and functioning of an X-ray photoelectronspectrometer .....	15
3.1 Schematic showing the principle of Optically Stimulated Electron Emission .....	37
3.2 Specular reflectance spectra of contamination on galvanized metal sheet .....	46
3.3 Ultraviolet spectra for abietic acid and a rosin flux .....	49
4.1 Ultraviolet Fiber Optic Spectrophotometer .....	58
4.2 Apparatus for determination of particulates and NVR .....	60
5.1 ESCA spectrum for copper switch contaminated with cutting oils.	64
5.2 ESCA spectrum for copper switch cleaned with dibasic ester .....	65
5.3 ESCA spectrum for copper switch cleaned by company with TCA.	66
5.4 ESCA spectrum for sputtered copper switch showing base metal composition .....	68
5.5 Comparision of ESCA spectra for heating coils cleaned with AL and NMP at condition R1 .....	69
5.6 Comparision of ESCA spectra for heating coils cleaned with AL and NMP at condition R2 .....	70
5.7 Overlaid raw infrared data for absorbance of oil on four cleaned metal coupons .....	73

5.8 Overlaid infrared spectra showing increasing levels of oil contamination present on cleaned metal coupons .....	74
5.9 Overlaid infrared absorbance spectra for identical oil in approximately similar amounts on two different steel coupons ...	75
5.10 Overlaid ultraviolet absorbance spectra for metal part soiled with cutting fluids in the contamination range of 2 to 7 mg./ square ft .....	77
5.11 Seven overlaid ultraviolet spectra taken at the same contamination level .....	78
5.12 Four overlaid ultraviolet spectra for increasing levels of power cutting fluid on steel coupons .....	80
5.13 SEC and SEP vs. number of factors for PLS cross validation of infrared data .....	86
5.14 Scores plot for first two factors for ultraviolet data .....	89
5.15 Scatter plot for predicted vs. actual contamination for PLS calibration model on ultraviolet data .....	94
5.16 SEC and SEP plotted against number of factors for PLS cross validation on ultraviolet data .....	95
5.17 Predicted vs. Actual contamination for infrared .....	99
5.18 Predicted vs. Actual contamination for ultraviolet .....	100
5.19 Predicted vs. Actual contamination for ESCA .....	101
5.20 Predicted vs. Actual contamination for gravimetry .....	102

## LIST OF TABLES

Table	Page
5.1 Carbon-to-Nickel ratios from ESCA analysis of nickel heating coils at factorial conditions .....	71
5.2 Results from gravimetric analysis of truck skin part coupons .....	81
5.3 PCR vs. PLS, variance captured for IR model .....	83
5.4 SEC and SEP for leave-a-group-out validation .....	85
5.5 SEC and SEP values for IR model .....	87
5.6 PCR vs. PLS, variance captured .....	88
5.7 SEC and SEP values for leave-a-group validation .....	92
5.8 SEC and SEP from final calibration model .....	93
5.9 Comparison of cleanliness levels from model and gravimetric testing .....	96
5.10 Cost vs. Prediction error for the four techniques .....	98

## NOMENCLATURE

Symbol/ Abbreviation	Meaning
AC	aqueous acidic
ACS	American Chemical Society
ADC	analog to digital
AL	aqueous alkaline
ATR	attenuated total reflection
CCD	charge-coupled device
CFC	chlorofluorocarbon
DBE	dibasic esters
EB	binding energy
ECD	electronic charge decay
Ee	photoelectron energy
EPA	Environmental Protection Agency
ESCA	electron scanning for chemical analysis
ERA	evaporative rate analysis
FTIR	Fourier transform infrared
h	Planck's constant
HC	hydrocarbon
HDA	head/disk assembly
IR	infrared
LPC	liquid particle count
MIL-STD	military standard

MSDS	material safety data sheets
NIR	near infrared
NMP	n-methyl pyrrolidone
NRC	nuclear regulatory c ommission
NVR	non-volatile residue
ORNL	Oak Ridge National Laboratories
OSEE	optically stimulated electron emission
P	ultrasonic power (watts/square cm)
PC	peak condition
PCB	printed circuit board
PCR	principal component regression
PEE	photoelectron emission
PLS	partial least squares
SAGE	solvent alternatives guide
SEC	standard error of calibration
SEP	standard error of prediction
t	time of cleaning (minutes)
T	temperature of cleaning (°C)
TCE	trichloroethylene
TE	terpene
THB	temperature, humidity, bias
UV	ultraviolet
w	spectrometer work function
XPS	x-ray photoelectron spectroscopy
X	matrix of spectral data
Y	matrix of concentrations

1,1,1, TCE

1,1,1 trichloroethane



# 1. INTRODUCTION

## 1.1 Problem Statement

During the fabrication of many types of equipment, soils and other residues are deposited on the parts. Cleaning the soiled parts is often a prerequisite for further processing operations like welding and painting, etc. In electronics applications, small amounts of contaminant dust or grease can be enough to render the product worthless. Similarly, equipment maintenance is an important factor in extending useful life, and parts-cleaning operations are usually included. Until the early eighties, hydrocarbon-based soils, grease and other organics were most often removed from metal parts by open-top vapor degreasing using trichloroethylene (TCE), a halogenated hydrocarbon. Since TCE and other halogenated hydrocarbons are now in the process of phaseout, manufacturers are testing alternative solvents for degreasing operations. The past few years have seen a glut of vendors espousing the merits of their respective alternative cleaning formulations. Industries are hence faced with the challenge of making the switchover to inexpensive, effective, and environmentally safe substitutes within the shortest time frame possible.

A variety of alternative cleaners can be used for parts-cleaning purposes, depending on the part's substrate composition and the contaminants to be removed. The effectiveness of the cleaning chemistry is enhanced by its use at optimum conditions of temperature, concentration, power, and time. Types of cleaning processes available



include ultrasonic cleaning, power washing, carbon dioxide snow, megasonics, and high pressure sprays [1]. The effectiveness of the cleaning step is best measured in terms of product performance. The level of cleanliness required for good performance is not always the maximum degree achievable. Metal parts can sometimes be cleaned "too well", leading to rusting on exposure to the atmosphere. In many applications, a certain degree of cleanliness below the maximum is enough to make the part acceptable for use in the next stage of processing.

Most industries employ some method of cleanliness testing before the parts are sent to the next stage of processing. These methods range from very crude qualitative visual inspection to highly sophisticated and expensive photoelectron spectroscopic techniques. The purpose of the research for this thesis was to develop an inexpensive, sensitive, and fast method to test parts surfaces for cleanliness. Dirty parts were obtained from industries in and around Tennessee who were trying to change over to alternate cleaning processes that do not use halogen-based solvents. These parts were cleaned with different classes of cleaning chemistries using ultrasonic and power washing equipment.

Analytical experiments were conducted using X-ray photoelectron spectroscopy (XPS, or ESCA) and infrared spectroscopy (IR) to test the parts. The results obtained were compared and correlated with results of cleanliness tests obtained by using portable ultraviolet (UV) fiber-optic instrumentation and a statistical model was developed. A predictive model was prepared for four different cleanliness testing methods: ESCA, IR, UV, and gravimetric testing. The predictions from these models were compared against actual values of contamination present on parts, and the

errors were related. The cost of each of these instruments was also taken into account when making final observations about the utility of each technique. The advantages and drawbacks of the ultraviolet method were studied. The expectation is that the experimental method used in this research can be extrapolated into the development of an easy-to-use instrument for on-the-spot quantitative testing of surface cleanliness.

## 2. BACKGROUND

### 2.1 Ozone Layer Depletion

The old adage that prevention is better than cure is especially relevant when it comes to environmental pollution. In recent years there have been highly significant advances in the understanding of the impact of human activities on the environment. This understanding has led to vigorous efforts to reduce the generation of pollution. The consensus is that pollution prevention should be the first step in protecting the environment. The next step is the recycling of any wastes that cannot be eliminated at source. Nonrecyclable waste should be treated in compliance with environmental standards and the waste remaining after treatment must be disposed of safely.

Ground-based and satellite observations of the lower stratosphere in the 1970s and 1980s showed a rapid decrease in global ozone levels. "Ozone holes" whose areas exhibited a quasi-biennial modulation were discovered in the polar Antarctic region [2]. It was found that periods of low ozone were accompanied by large increases in surface ultraviolet radiation in the Antarctic. Contemporary studies in the Arctic revealed that low-ozone periods there were concurrent with the presence of elevated levels of reactive chlorine. Further research led to strengthening of the evidence that the Antarctic ozone holes are also primarily due to chlorine- and bromine- containing chemicals [3].

On September 16, 1987, an international agreement, the Montreal Protocol, was signed by officials from 73 countries to assess and control



atmospheric ozone levels. At the Protocol's renegotiation in London in 1990, the now 94 parties to the Protocol agreed to limit the production of chlorofluorocarbons (CFCs) to 15 percent of 1986 levels by 1997 and to aim for complete phaseout by the year 2000. Tentative deadlines were also drawn up for new substances to be controlled: carbon tetrachloride and methyl chloroform. The Protocol went into force in January 1991, and the first reassessment reports were published in October 1991. Ozone depletion was found to be worse than expected: 3 percent versus the original 1 percent, and the Antarctic hole was discovered to be bigger and longer lasting [4]. However, the good news was that improved ozone layer observation techniques were now available, and chemical producers had started announcing alternatives for harmful chemicals. CFC production was down to 40 percent below 1986 levels, and no solvent issues were identified as impediments to the proposed 1997 phaseout. Worse news about the ozone layer was reported during the second negotiation in Copenhagen in 1992: 6-8 percent depletion was observed in the polar regions and the mid-latitudes were found to be affected [5]. CFC production was, however, being reduced at a more rapid rate than anticipated, and the accelerated phaseout schedule looked promising.

In the United States, the Environmental Protection Agency (EPA) sets guidelines and oversees efforts aimed at reducing pollution. In February 1991, EPA launched the voluntary 33/50 program, which is aimed at reducing releases and off-site transfers of 17 toxic chemicals including some ozone-depleting substances by 50 percent by the end of 1995 [6]. Companies were asked to voluntarily examine their chemical processes and implement cost-effective pollution prevention practices for these

chemicals. On December 3, 1991, the EPA was petitioned by environmental groups to invoke the emergency provisions under the Clean Air Act, Section 303, and the accelerated rulemaking provisioned under Section 606. In response, EPA scheduled phaseout for halogenated hydrocarbons for 1992, for CFCs by 1995, and for hydrochlorofluorocarbons (HCFCs) by 2000. Included in this list of chemicals slated for accelerated phaseout were several halocarbons, which have been identified in scientific studies as being major contributors to stratospheric ozone layer depletion.

## **2.2 Alternate Cleaning Techniques**

A variety of processes and chemistries are utilized in industrial metal parts-cleaning operations. The specific method applied depends on a number of factors. Important among them are the metal substrate involved, the type of soil adhering to the parts, the part geometry and size, the production rate of the parts, the ability of the parts to withstand high pressures, the degree of cleanliness required, and the next processing stage to which the parts are subjected. The chosen cleaning agent must be compatible with the metal, be able to remove the contaminant (given proper agitation), and leave very little, or easily removable residue on the parts. The cleaning equipment must account for part size and possible contortions in part structure, provide enough agitation, and be able to handle large throughput rates. These are purely performance considerations; cost factors like price of cleaner, equipment, and maintenance must also be taken into account, along with environmental requirements of waste reduction and recycling.

### 2.2.1 Alternate Cleaning Chemistries

Cleaners are often classified based on their compatibility with water as aqueous, semi-aqueous, or non-aqueous [7, 8]. Aqueous agents, further subdivided into acid, neutral and alkaline types, are among the most widely used alternates. Aqueous cleaners generally consist of water mixed with special agents like detergents, surfactants and builders to assist in soil removal. These agents help to bolster the cleaning capacity of water, which on its own is not particularly effective on non-polar contaminants, by enhancing properties like wettability, solubilization, foaming, and emulsification. Among the inorganic constituents of aqueous cleaners are phosphates, borates and chelators, meant to provide water softening and corrosion protection. Organic components include detergents, emulsifiers, wetters, and defoamers. These compounds, combined properly, perform the water-based cleaning operation. The choice of chemicals added to the aqueous base depends on the type of soil and type of part, which dictate cleaning time, temperature, and cleaner concentration. Acid cleaning helps in splitting of soils, and is recommended for removal of metal oxides and scale. Acidic cleaners generally contain toxic compounds, usually require inhibitors, and are not suitable for removal of soaps and synthetics. Alkaline cleaning is generally economical and versatile, being able to operate over a wide temperature range for a variety of substrates. Its further advantages are low toxicity and recyclable constituents, while its negatives include difficulties sometimes posed during rinsing and foaming and incompatibility with certain electrical components.



Hydrocarbons, terpenes, pyrrolidones, and esters are classified as semi-aqueous cleaners. Terpenes, derived from pine and citrus sources, have excellent solvency characteristics. These have to be balanced with their low flash points and pleasantly sickening odor which might require special considerations in equipment design. A rinse stage is usually required after a terpene-based wash. Hydrocarbons, which might also have low flash points, are usually combined with a surfactant and rust inhibitor. They are effective in removing various oils, greases, and waxes. Recycling is generally an option, and waste may be incinerated. Dibasic esters (DBE) and n-methyl pyrrolidone (NMP) are gaining acceptance as suitable alternatives. Additives are often added to these compounds and some compositions are dilutable. Semi-aqueous solvents have lower surface tensions than water and are hence better suited for applications involving surface irregularities containing trapped contaminant.

Several non-conventional cleaners are currently in various stages of testing and implementation as safe and reliable alternatives to CFCs. Among them are supercritical fluids, carbon dioxide snow, particle blasting and laser ablation. These methods are applied in specific instances where traditional methods fail or are not viable due to cost considerations.

### **2.2.2 Alternate Cleaning Technologies**

Until now, open-top vapor degreasing has been the most commonly used method for cleaning. The part is introduced into a chamber saturated with the vapors of a hydrocarbon like 1,1,1 trichloroethane distilled from a vat of the boiling solvent. The vapors condense on the cool part and flush

away the solvent as the condensed solvent drips down. Uncontrolled vapor degreasers of this kind can release as much as 0.3 lb. of solvent per square foot of degreaser opening per hour [9]. Modifications such as primary cooling coils, higher freeboards, and reduced chiller temperatures help reduce emissions. Alternate processes must be designed to have very low emissions.

A number of alternate methods have been proposed in the past few years although some of these have been in use for many years, albeit on a small scale. Alternates processes can be classified as liquid, mechanical, and advanced. Liquid processes, as the name suggests, provide the agitation and environment for effective detergent and solvent performance. Low- and high-pressure sprays, power washers, immersion cleaning, steam cleaning, ultrasonics, and megasonics are examples of this class. Brushing, wiping, abrasives, and carbon dioxide pellets are mechanical processes. Advanced processes, often expensive and not freely available, include carbon dioxide snow, plasmas, laser ablation and supercritical fluids.

Soak tanks are used when a particular contaminant needs extended periods of exposure to soften or dissolve soils. This can be used as a pre-cleaning step to allow the chemicals to break down soluble contaminants, and can be used in conjunction with a hot alkaline stripper for paint removal or similar applications. Recirculation and filtration systems are used to avoid excess soil loading in stand-alone soak tanks. Agitation can be provided in tanks by pumping, mechanical stirring, air pressure stirring, and platform or workpiece rotation. A typical closed loop aqueous/semi-



aqueous washing system with wash and rinse stages, followed by membrane filtration and recycling is shown in Figure 2.1.

Low pressure spraying is an effective means for gross removal of loose solid and liquid contaminants. The system usually consists of a tank, spray wand, liquid reservoir, pump and filter, and can be used as a rinse cycle within a larger sequence of cleaning steps. The operating pressures are below 200-300 psi, and decontamination is based mostly on kinetic energy and not on chemistry. The system can be optimized through better nozzle design, control of liquid flow rates, use of non-foaming solvents, and use of effective spray patterns. High pressure sprays are especially useful in particle removal and cleaning of blind holes. They are generally used when higher levels of cleanliness are required and usually operate at pump pressures above 500 psi. Water is often used as the spraying liquid since direct impingement causes most of the cleaning. A variety of spray washing systems like carousel, monorail, rotary drum, belted spray and cabinetized spray washers are in use. Carousels are continuous-cleaning systems where parts are placed on a revolving turntable and processed through wash, rinse, and blow-dry cycles. A single operator can oversee the process, and cleaned parts are returned to him once the process is complete. Rotary drum systems are used for large volumes of small parts with non-critical surfaces. Parts are immersed in a hot washing solution and tumbled through a series of baths prior to a forced-air drying cycle. Belted spray washers have a mesh belt carrier that delivers parts through a series of spray chambers, where they are forcefully impinged upon by a chemical solution through use of strategically located spray nozzles. This kind of system can be easily integrated into existing production lines.

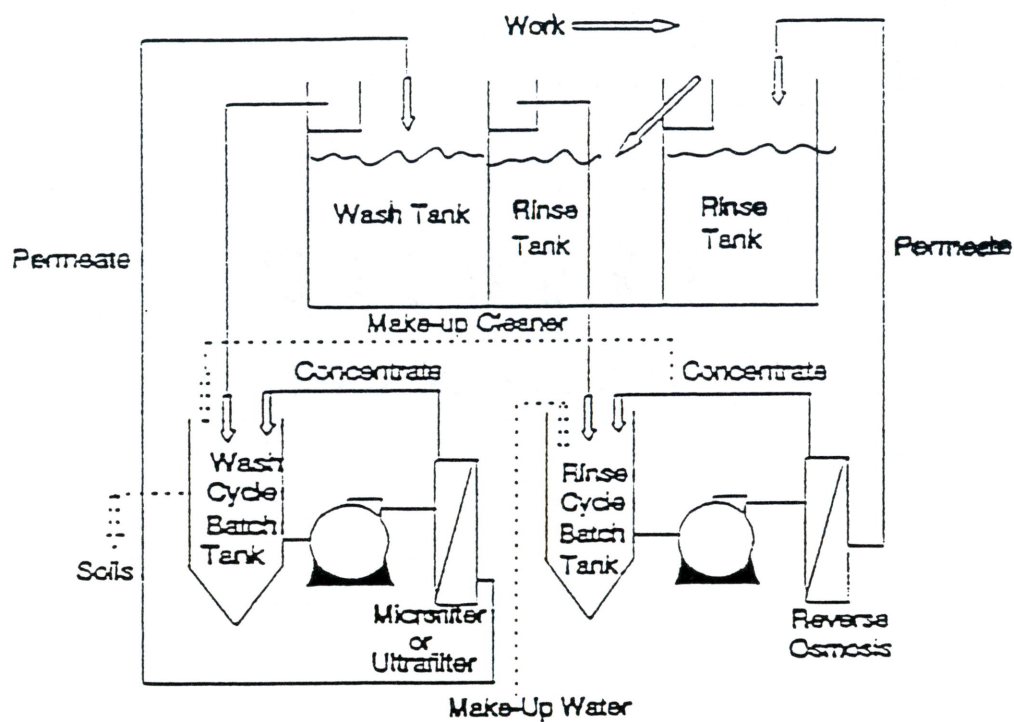


Figure 2.1 A typical cleaning and recycling closed loop for aqueous and semi-aqueous formulations [8].

Overhead conveying systems are designed for continuous, high-volume applications. They function as a self-contained, single-operator, continuous loop system.

Ultrasonic equipment uses sound waves of frequencies more than about 18 kHz for cleaning purposes [10]. At sufficiently high amplitudes, "rupture of liquid" occurs in areas of high negative pressures (rarefaction). "Cavitation bubbles" are formed at the sites of rupture. As the wavefront passes and the pressure becomes positive (compression), the bubbles begin to oscillate and finally implode. These implosions cause shock waves to be propagated from the rupture sites. Temperatures greater than 10,000 °F and pressures greater than 10,000 psi are generated at these sites. This formation and implosion of bubbles generates a scrubbing or cleaning action which is impossible to achieve through other mechanical means [11].

Ultrasonic tanks are normally used as part of a multi-stage cleaning system, and are good for achieving all levels of cleanliness. A transducer and a generator are required to introduce ultrasonic energy into the system. High frequency electrical oscillations produced by an electric generator are fed to a transducer which is applied to two piezoelectric elements in the transducer which vibrate. After amplification, these vibrations are directed into the liquid through the radiating plate by the resonant masses of the transducer. Transducers can be mounted in the metal tanks at the bottom or on the sides, or directly immersed into the liquid [12]. If temperature is an important parameter, magnetostrictive transducers may be used in place of piezoelectric ones. Properly designed fixtures help avoid the casting of "shadows" or blocking the action of sonic waves.



The ultrasonic cleaning mechanism is affected by a variety of factors. Research into the influence of the physical properties of the liquid and the frequency and intensity of the sound field have led to the formulation of some basic guidelines for efficient cleaning [13-15]. Chief among these guidelines is the necessity to operate at low frequencies (18-44 kHz) and elevated specific acoustic powers (2.5-10 W/cm<sup>2</sup>). Erosion also depends on temperature, solvent used, material hardness, surface finish, and cleaning time. Studies have shown that temperature is usually the most important operating variable [16]. This holds true as long as the boiling point of the liquid is not approached. Near the boiling point, the negative pressure causes boiling, hence little or no cavitation takes place.

## **2.3 Spectroscopic Methods**

Many spectroscopic methods have been used to characterize part cleanliness levels. These include X-ray, infrared, and ultraviolet techniques. A brief description of these methods is given below.

### **2.3.1 Electron Scanning for Chemical Analysis (ESCA or XPS)**

Electron spectroscopy has found increasing use in the last two decades as a means of studying chemical systems. ESCA works in the following manner: An X-ray beam irradiates a target sample; the ejected electrons enter the spectrometer and are separated according to their energies or momenta; they strike a detector and are counted; and the data is suitably stored [17].

Figure 2.2 shows the components of a typical ESCA system. The excitation device may be an electron gun, an X-ray tube, or a gas discharge lamp. The target may be a solid, frozen, condensable vapor, or a gas which is allowed to fill a volume that can be exposed to radiation. In an X-ray tube, characteristic X-rays are produced by bombarding a suitable target with electrons. Vacancies thus created in the inner shells are filled with atomic electrons, and X-rays are produced as a result. The threshold energy for the process is the binding energy of the inner shell electron. The two most important sources used in photoelectron spectroscopy are the characteristic  $K\alpha$  X-rays of magnesium (Mg) and aluminum (Al). These yield the narrowest K X-ray lines that can be practically obtained.  $K\alpha$  X-rays occur as a result of a radiative transition in which a K vacancy is filled by an electron from the L shell. The intensity of the X-rays produced depends on the voltage and current of the electron beam striking the anode [17, 18].

Solid targets are usually mounted in a fixed position as close to a photon source or an entrance slit as possible, so that the ejected electrons are transmitted into the analyzer with high efficiency. For surface studies, a high vacuum is required. Several samples can be introduced into the spectrometer at the same time. The photoelectric effect is a dipole interaction in which all the energy of the photon is expended in the ejection of a bound electron. Photoelectron spectroscopy is used to determine the binding energies of the atomic and molecular orbitals, using the following relationship:

$$EB = h\nu - E_e + w \quad (2.1)$$

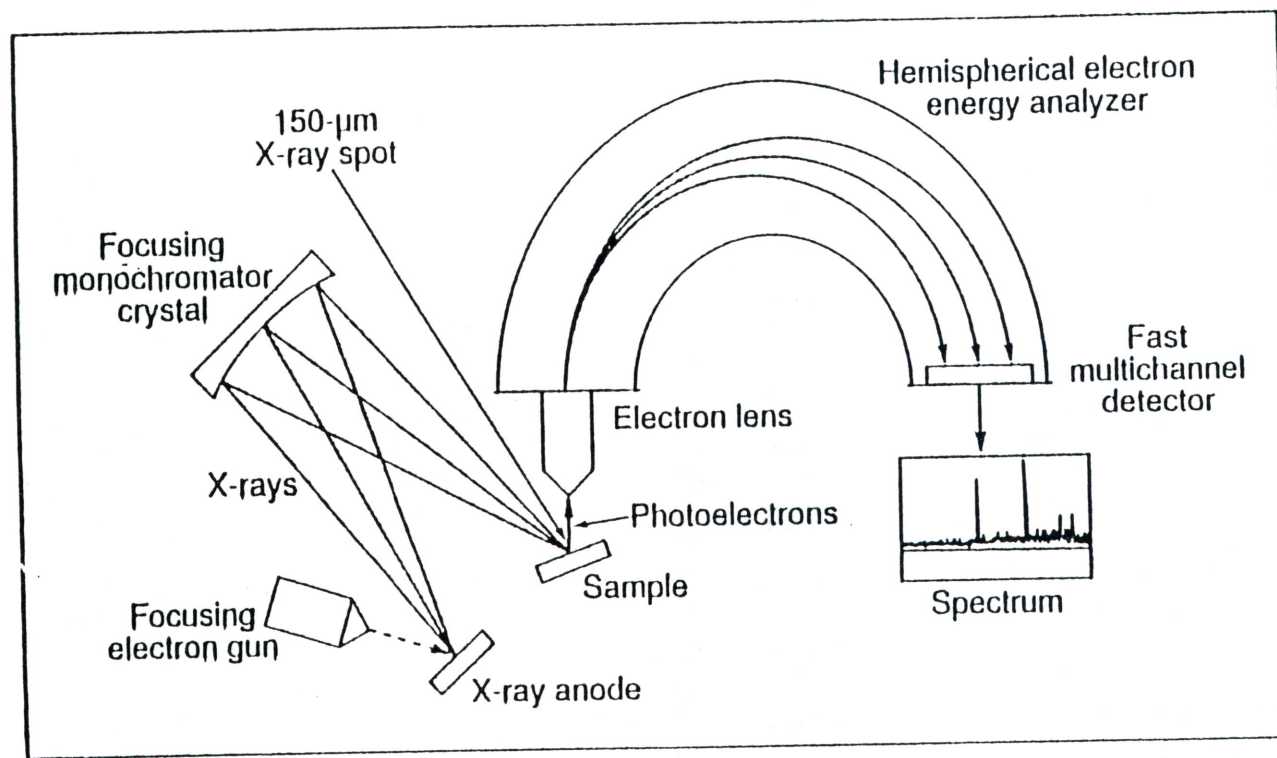


Figure 2.2 Schematic showing the basic components and functioning of an X-ray photoelectron spectrometer [17].

where EB is the binding energy,  $h\nu$  the photon energy,  $E_e$  the photoelectron energy and  $w$  the spectrometer work function. The binding energy for a given molecular or atomic orbital is the difference in total energy between the initial and final states of the system in which one electron has been removed from the given orbital. As a result of photoionization, the resultant ion will find itself in one of a number of final possible electronic states. The energy of the photoelectron is governed by the difference in total energies of the initial and final states. The width of the photoelectron line is related to the lifetime of the final state according to the Heisenberg uncertainty principle,

$$\Delta E = h/Dt \quad (2.2)$$

where  $Dt$  is the mean lifetime of the final state.

Each element has a different binding energy associated with the removal of an electron from an orbital. The detector counts the number of electrons, and a plot can be obtained of the number of electrons per energy level versus the binding energy of the electrons. Peaks corresponding to the elements present in the sample are obtained at the binding energies characteristic of the respective elements. For measuring the amount of organic contamination on the surface of a metal sample, the ratio of the carbon peak area to the area of the dominant metal peak is taken.

Developments in the last 20 years have led to steady refinement and improvement in the instrumentation for surface electron spectroscopies [19]. These include improved sample handling, better source designs, high-resolution and high-efficiency analyzers, new detector designs, and better



computer-control and data-processing techniques. It is foreseeable that surface analytical information will be used to define device specifications and differentiate competing technologies. ESCA measurements usually yield reliable, accurate data. Limitations include the specific size and shape of the sample to be used in the analysis (requires a small flat surface, not always possible), the cost, and additional analysis time required.

### **2.3.2 Infrared Spectroscopy**

The electromagnetic spectrum of light is divided into distinct regions defined by specified wavelength ranges. The infrared region is defined as the portion of the spectrum from 700 nm to about 500,000 nm. A wealth of information can be obtained by analysis in this region and for years it has been the most investigated region of the light spectrum. Subdivisions of this region are called near infrared (700 nm to 2,500 nm), mid infrared (2,500 nm to 5,000 nm) and far infrared (5,000 nm to 500,000 nm). Energy transitions from the ground state to the first excited state are called fundamental vibrations. Transitions to second or higher states are called overtones. In the near infrared (NIR) region, the absorption bands are weaker and the peaks are not very sharp. The transitions in this region are of higher frequency and are attributed to overtones and combinations of the fundamental molecular vibrations. NIR offers more flexibility as to the selection of overtones for analysis. The mid infrared region shows sharper absorption peaks which result from fundamental vibrations and first overtones [20]. The sharp functional group peaks lend themselves to simpler analysis. The high sensitivity in this region requires more careful



handling of samples and use of appropriately diluted or thin samples. The far infrared region embraces a large number of conventional types of vibrations--the stretching of bonds involving heavy atoms as well as bending vibrations in a large range of inorganic and organic molecules. Absorption bands in the far infrared are sometimes very broad.

### **2.3.3 Ultraviolet Spectroscopy**

The ultraviolet region of the electromagnetic spectrum spans the 200 nm to 360 nm range. Characteristic of this region are the strong and broad absorption bands and both atomic and molecular transitions lead to absorption in this region. A discussion of ultraviolet spectroscopy can be found in [21, 22]. Due to the broad and less precise bands in this region, it is difficult to identify absorbers in the ultraviolet. Ultraviolet techniques are often used to test for purity, rather than for identification purposes. The ultraviolet range of 200 to 360 nm can be especially useful, since water does not have any absorption above 200 nm. Chromophore functional groups absorb in this region and are typical of the types of structures encountered in organic contamination control. In addition to aromatics and olefins, a very large range of molecules and ions absorb in this region [23].

### **2.3.4 Sampling Methods**

Transmission spectroscopy takes advantage of the transparent nature of the medium under investigation to measure the absorption of dissolved substances as a function of wavelength. This method is not

suitable for colloidal systems where light scattering phenomena result in substantial energy losses, and for determining the absorption spectra of substances adsorbed on solid surfaces. Reflectance spectroscopy is well suited to make contributions in these areas. Hardy [24] developed the first recording reflectometer using an integrating sphere, which permitted collection of diffusely reflected light but excluded the undesirable specular component.

Radiation reflected from a finely divided solid consists of a specular reflection component and a diffuse reflection component. Specular, or regular, reflection arises from reflection occurring at the surface of the system with no transmission through it. Diffuse reflection results from radiation that has penetrated and subsequently reappeared at the surface of the system following partial absorption and multiple scattering within the system. Since these are complementary phenomena, the elimination of the regular reflection component is of importance in the design of diffuse reflection equipment.

The Kubelka-Munk [25, 26] development is the most general theory treating diffuse reflectance. For an infinitely thick opaque layer (in practice, a few mm thick), the equation is written as,

$$F(R_{\infty}) = (1 - R_{\infty})^2 / 2R_{\infty} = k/s \quad (2.3)$$

where  $R_{\infty}$  is the diffuse reflectance of the layer relative to a non- or low-absorbing standard such as magnesium oxide,  $k$  is the molar absorption coefficient of the sample, and  $s$  is the scattering coefficient. For weakly absorbing materials, where the regular reflection component is small, it

has been confirmed that  $F(R_-)$  varies linearly with  $k$ , for constant  $s$ . In this form, the Kubelka-Munk equation is comparable to the Beer-Lambert law of transmission spectroscopy.

The above mentioned transmittance and diffuse reflectance measurements can be combined to make what are known as "transflectance" measurements, in which the radiation incident on the sample is partially reflected and partially absorbed. Colloids and suspensions are often analyzed in the manner. Emission spectroscopy is particularly useful in the study of samples at very high temperatures, remote samples, or very thin films. The sample being studied is usually a gray body, and a black body is generally taken to be the reference. In emission spectroscopy, the emitting sample becomes the source for the Fourier transform infrared (FTIR) instrument. Other sampling methods commonly in vogue include photoacoustic spectroscopy, attenuated total reflection (ATR) spectroscopy, and Fourier far infrared spectroscopy.

## **2.4 Multivariate Data Analysis Techniques**

Spectra obtained from spectroscopic methods contain absorbance levels at different wavelengths. Since the absorbance spectra in the ultraviolet region is in the form of broad bands, information regarding concentrations or other desired properties cannot be determined by choosing a single wavelength [27, 28]. Hence multivariate techniques like PCR and PLS have to be used to relate absorbance to the property of interest.



Earlier approaches like classical least squares (CLS) and inverse least squares (ILS) were based on an initial qualitative understanding of the spectral features, and the identification of a minimal set of appropriate wavelengths for analysis [29, 30]. This at times leads to the inclusion of outliers which are not representative of the data, causing an inaccurate and extremely sensitive model to be developed. Full spectrum methods like PCR and PLS relate the spectral information to the property of interest, while being able to detect outliers and minimize the effect of interdependence among the regressing variables. They are based on the principle of reduction of the dimensionality of the original data into a smaller dimensional frame which still accounts for most of the useful information.

#### **2.4.1 Least Squares Methods**

Classical and inverse least squares methods are regression methods based on multiple linear regression techniques wherein the average of the squared residuals is minimized.

##### **Classical Least Squares**

The classical least squares method is based on Beer-Lambert's law, according to which absorbance is directly proportional to concentration of species. For a multicomponent mixture, in matrix notation, the relationship between the absorbance and the concentrations is given by

$$A = CN + E \quad (2.4)$$



where  $A$  is an  $m$  by  $n$  intensity matrix of the calibration spectra of  $m$  samples at  $n$  wavelengths,  $C$  is an  $m$  by  $p$  matrix of concentrations with  $m$  samples and  $p$  analytes,  $N$  is a  $p$  by  $n$  matrix of pure analyte spectra coefficients, and  $E$  is the matrix of residuals. Each column of  $N$  represents the pure spectrum at a particular wavelength of the constituents at unit concentration and unit path length. A simple least squares estimate of  $N$ ,  $N^*$ , is given by

$$N^* = (C'C)^{-1}C'A \quad (2.5)$$

This requires that the columns of  $C$  be linearly independent so that the matrix  $C'C$  is invertible. Using the above estimate for  $N$ , concentrations of constituents in an unknown sample can be predicted using

$$C^* = (N^*N^{*'})^{-1}N^*A_{\text{new}} \quad (2.6)$$

where  $C^*$  is the predicted value of  $C$  and  $A_{\text{new}}$  is the new measured absorbance matrix. This method requires that all the spectral data including those corresponding to interfering constituents be used in the calibration. It also requires that both  $(N^*N^{*'})$  and  $(C'C)$  be invertible.

### **Inverse Least Squares**

This method is based on the inverse Beer-Lambert Law model. This assumes that the concentrations are dependent variables and are directly proportional to the absorbance. The calibration for this case is given as

$$C = MA + E \quad (2.7)$$

where  $C$  is a  $p$  by  $n$  matrix of analyte concentrations,  $M$  is a  $p$  by  $m$  proportionality matrix between  $A$  and  $C$ ,  $A$  is an  $m$  by  $n$  matrix of absorbances, and  $E$  is a  $p$  by  $n$  residual matrix. The proportionality matrix is calculated during the calibration step. A least squares estimate of  $M$ ,  $M^*$ , is given by

$$M^* = CA'(AA')^{-1} \quad (2.8)$$

The concentrations of the unknown samples,  $C^*$ , can now be estimated as

$$C^* = M^*A_{\text{new}} \quad (2.9)$$

where  $A_{\text{new}}$  is the measured absorbance matrix of the unknown samples.

#### 2.4.2 Principal Component Regression

When the spectral data are in the form of broad, overlapping peaks a great deal of redundant information is present and a simple least squares solution although obtainable, would turn out to be unstable. Principal component regression takes care of the redundancy by explaining the variation in the absorbance data set in terms of a smaller number of variables (principal components) by eliminating the redundancy in the data among the wavelengths. Much of the redundancy in the information can be attributed to interdependence among the spectra at different

wavelengths. The PCR method is based on attempting to extract the optimal number of factors such that the residual matrix contains only random noise and not any essential information.

The variance in the  $X$  data set is expressed in terms of a much reduced set of mutually perpendicular principal components. In this linear regression method, a calibration model is first constructed between spectral data and a well prepared samples of known concentration levels. This is expressed as

$$Y = X\beta + F \quad (2.10)$$

where  $\beta$  is an  $n$  by  $p$  matrix of regression coefficients and  $F$  is an  $m$  by  $p$  matrix of residuals of  $Y$ .  $X$  and  $Y$  contain the spectral responses and contamination concentration levels respectively. A singular value decomposition (SVD) approach of performing PCR was chosen as described in [32]. The first step is to obtain the singular value decomposition of the matrix  $X$  as

$$X = USV' \quad (2.11)$$

where the columns of  $U$  are the left singular vectors of  $X$  which are also the eigenvectors of  $XX'$ ,  $S$  is a diagonal matrix with positive, descending elements (singular values) being the square roots of the eigenvalues of  $X'X$ , and the columns of  $V$  are the right singular values of  $X$  which are also the eigenvectors of  $X'X$ .

In spectroscopic data, a great deal of collinearity exists, so not every wavelength variable represents a linearly independent direction. Since absorbance values at different wavelengths may provide essentially the same information, a robust least squares solution cannot be obtained. To eliminate collinearity PCR removes components with zero or very small singular values and reduces the dimension of the data. This is expressed in terms of "reduced" matrices of rank  $r$  (usually,  $r \ll \min(m,p)$ ), as

$$X_r = U_r S_r V_r' \quad (2.12)$$

The  $X_r$  matrix has a rank much lower than before but it still retains most of the information contained in the original matrix  $X$ . The small but non-zero singular values are assumed to be manifested by random error and are assumed to have no correlation to the contamination levels. Thus data represented by the principal components with the smaller singular values are to be discarded. When reducing data, a careful assessment must be made of the number of principal components that must be included in the model. Including too few might mean leaving out some important information (underfitting), while taking too many could mean a chance of building the model with noise (overfitting) and hence highly susceptible to a small change in the spectral reading. The reduced matrices are now used to obtain an estimate of the regression coefficient matrix using the pseudoinverse of  $X_r$ .

$$X_r^+ = V_r S_r^+ U_r' \quad (2.13)$$

as



$$\hat{\beta} = X_r^+ Y \quad (2.14)$$

where  $X_r^+$  is obtained by inverting the singular values. The resulting  $\hat{\beta}$  is used for prediction purposes as in  $Y^* = X_{\text{new}} \hat{\beta}$ . PCR methods account for the full spectrum and have a signal-weighted averaging effect.

In PCR, the dimension of the data is reduced by taking only the  $X$  matrix into account. The partial least squares regression method performs a similar task but uses both  $X$  and  $Y$  matrices. PCR method can utilize the full spectra resulting in a signal averaging effect. Noise and interdependence are eliminated by casting away smaller singular values; however if the analyte has a very weak but independent signal it is possible that its spectral response might be discarded during the PCR procedure as noise.

### 2.4.3 Partial Least Squares

In the partial least squares method the reduction of the dimensionality of the raw data is based on both the  $X$  and  $Y$  matrices and not on the  $X$  matrix alone [28,29, 31-33]. In PCR it is assumed that the discarded variables have no correlation to the  $Y$  matrix and the dimensionality is accordingly reduced. However, essential information might be lost by the removal of components that explain a relatively low amount of variability in the  $X$  data, but which might be highly correlated to the  $Y$  data variation. PLS accounts for this by choosing principal components which line up not with the  $X$  data variation, but with the variation  $Y$  data as well, thus ensuring that no essential regressable

information is lost. PLS components are selected to give maximal reduction in the covariance  $X^TY$  of the data.

A separate model is created for both  $X$  and  $Y$  matrices [33]. The equations representing the PLS method are generally to be expressed as

$$X = TP' + E \quad (2.15)$$

$$Y = LQ' + F \quad (2.16)$$

where  $X$  is of size  $m$  by  $n$ ,  $Y$  is of size  $m$  by  $p$ ,  $T$  and  $L$  are the scores matrices for  $X$  and  $Y$  respectively and are of size  $m$  by  $r$ .  $P$  and  $Q$  are the loadings matrices and are of size  $n$  by  $r$  and  $p$  by  $r$  respectively.  $E$  and  $F$  are residual matrices of sizes  $m$  by  $n$  and  $m$  by  $p$  respectively. This kind of decomposition aims to preserve the maximum correlation between  $X$  and  $Y$ .

In PLS method the columns of  $X$  and  $Y$  can not be orthogonal at the same time. Depending on the algorithm (PLS1 vs. PLS2), either the columns of  $T$  are orthogonal or the columns of  $P$  are orthogonal. Useful qualitative information can be obtained from the full spectrum PLS methods. Spectral features that are positively and negatively correlated with the analyte contaminations are indicated by the first PLS loading spectrum obtained from the first column of matrix  $P$ . If we have a physical property instead of contamination levels, its correlation to structural features can be obtained. Another advantage of the PLS technique is that it can be used even when unknown spectral interferences are present or there are analyte interaction effects in the system.

The number of latent variables to be used,  $r$ , is obtained from cross validation procedures. The reduced  $X$  and  $Y$  are then correlated and the resulting regression coefficients are used for predictions. In the non-linear iterative partial least squares (NIPALS) algorithm, the columns of the scores matrix  $T$  are orthogonal, but not those of  $P$ . Several other algorithms exist for decomposing the  $X$  and  $Y$  matrices. These include algorithms by Martens [34], the SIMPLS method [35] and the SVDPLS method [36] proposed by Wang *et. al.* The SVDPLS method was shown to be up to ten times faster than the traditional iterative NIPALS method and have better numerical properties. After choosing the optimum number of latent variables after cross validation, the reduced  $X$  and  $Y$  are used for prediction.

#### 2.4.4 Evaluation of Regression Results

MATLAB [37] software was used for the development of the calibration model using a SVD-based regression approach. Prediction was done on both calibration and prediction samples. Goodness of fit is evaluated by three parameters--the SEC, the SEP and the PRESS. The standard error of calibration (SEC) was calculated as

$$SEC = \sqrt{\frac{\sum_{i=1}^{nc} (y_{i,c} - y_i)^2}{(nc - 1)}} \quad (2.17)$$

where  $y_{i,c}$  is the property of sample  $i$  estimated from the calibration model and  $nc$  is the number of calibration samples. The quality of a given

calibration model can be judged by calculating the SEC which represents a quantification of calibration errors. The standard error of prediction (SEP) is given by

$$SEP = \sqrt{\frac{\sum_{i=1}^{np} (y_{i,p} - y_i)^2}{(np)}} \quad (2.18)$$

where  $y_{i,p}$  is the property of sample  $i$  predicted from the model,  $y_i$  is the known property, and  $np$  is the number of prediction samples. The number of factors to be included in the final calibration model is determined by the values of the SEP. The model with the least SEP value is chosen finally for calibration and the unknown samples are predicted using this model. Low values of SEC and SEP show that a good fit has been obtained. The SEP value is the best indicator of the ability of spectral data to predict the contamination concentration levels. An alternate method of determining goodness of fit is by evaluating the predicted residual sum of squares which is given by

$$PRESS = \sum_{i=1}^{np} (y_{i,p} - y_i)^2 = (SEP)^2 (np) \quad (2.19)$$

where  $y_{i,p}$  is the predicted value of concentration of sample  $i$ . Since the PRESS value represents the deviation of the predicted values from the actual concentrations, it is a good measure of the accuracy of the model. The model with the minimum PRESS value can also be chosen as the calibration model.



### 3. LITERATURE REVIEW

#### 3.1 Testing Surfaces for Cleanliness

Surface identification is accomplished using a myriad of techniques, ranging from the inexpensive and very crude to the expensive and sophisticated. Unsophisticated methods like the wipe test or the water break test can be easily done on the production floor. These tests are, however, very subjective and it is difficult to obtain consistent results from them. On the other hand are the laboratory analytical inspection techniques, many of which need skilled technicians for operation and analysis of results. These instruments are usually not portable and require that tests be conducted in a laboratory, instead of the more convenient and quicker shop floor testing. The instrument's degree of sophistication is, unfortunately, not correlated to the success of the subsequent operation, and these analytical methods often yield unreliable results. Thus each method has its strengths and weaknesses and their identification can enable their use in particular appropriate applications. Following is a brief description of the more popular methods:

Visual inspection is the earliest and most obvious method for cleanliness testing. Cleaned parts are examined visually for the presence of residual contaminant. If a grease film or particulate material is visible, the part is sent back for recleaning. Parts that appear clean to the naked eye are cleared for further operations. A standard method of inspection of painted surfaces is based on the comparison of the change in gloss of a cleaned panel to that of a standard panel [38]. In the semiconductor industry,

microcontamination on chips is examined using high resolution microscopy. The decision on the degree of cleanliness is a very subjective one, depending entirely on the person conducting the test. Nevertheless, this test is still widely used in cases where gross contamination removal is the primary objective.

Wipe testing, the second-oldest technique, is a simple qualitative test detecting the presence of contaminant. Dirty panels are cleaned and then wiped with a white cloth or tissue. The presence of soil on the cloth or tissue is indicative of poor cleaning. The amount of visible dirt is used to qualitatively specify different levels of cleanliness. Weltman and Evanoff [39] used the water break, ultraviolet light and Nielson methods to evaluate the cleanliness of aluminum panels. They found that a simple wipe test as described by Spring and Cohen [40] detected the presence of inorganic residues on vendor-supplied materials that were not easily identified using the other three methods. This test depends to a certain extent upon the amount of pressure exerted during the wiping step and the surface area of the cloth or tissue subject to contact by rubbing. Better results have been observed when the surface in question is wet [41, 42].

The classical water break test is probably the most widely used qualitative test in industry. It is used to test for the presence of oils and grease films. A clean metal has a hydrophilic surface, that is, one that can retain a film of water. The part is dipped in water, or water is trickled on the part, and a break in the water film is revealed in the soiled area. If the water drains intact, the film having persisted for a 30-second drainage period, the surface is assumed to be clean. This simple-to-use test has its advantages and drawbacks. Contamination in the form of traces of

surfactant or soap cannot be easily detected, because they promote the flow of water on the surface. Inorganic residues which are wetted by water cannot be detected. While this test is, in general, nondestructive, the use of warm water can lead to rusting. The results from the water break depend to a great extent upon the thickness of the water film. This factor is a very difficult one to control, and false results can be obtained due to bridging of the residues. To avoid this pitfall, a modified version of this test which involves a mild acid dip and a water rinse before the break test, is sometimes employed [43]. Thompson *et. al.* [44] conducted water break experiments at Oak Ridge National Laboratories (ORNL) which revealed that water does not wet certain metal oxide surfaces. In fact, the more these surfaces are cleaned, the quicker the water beads. This test is quick, simple, and has been found to yield very good results in electroplating operations [45].

The Nielson test is a fairly well-known method that employs two tests on 10 individually processed panels to determine the time required for each to be cleaned [46, 47]. The cleaned panels are tested with the water break test. They are then immersed in a copper sulfate solution (typically 140 gm of copper sulfate and 30 cm<sup>3</sup> per gallon of water). Copper is deposited by chemical activity on the clean areas, forming a semi-bright coating free of spots. This is called the acid copper test and is generally used for ferrous panels. Panels that do not pass this test are cleaned and tested again. An average of the cleaning times required to clean the 10 panels is taken as a measure of the effectiveness of the cleaning solution.

The atomizer test is very sensitive when compared to tests like the water break test. Test panels are first cleaned with the respective solvents



and then dipped in acid. The wet panels are dried and then placed in a vertical position. An atomizer is used to spray a blue dye solution on the panels. Spraying is stopped just before the dye begins to run, and the panels are placed horizontally. The pattern that forms on the surface is then sealed by application of heat. A grid is placed over the panels and the number of clean squares on each is counted. The cleaning index is taken to be the averaged percentage of the total area that appears to be clean. The spray test [48] is similar to the atomizer test and the results are also expressed in terms of a semi-quantitative index.

More sophisticated variations to the water break test are in vogue. A contact angle goniometer is used to measure the angle made by a drop of water with the cleaned surface. The presence of oil on the surface leads to a decrease in the surface tension of the surface. An absolutely clean surface would ideally have a contact angle of  $0^\circ$ , and a very dirty surface an angle of  $90^\circ$ . Modifications to the test include measuring contact angles for a series of liquids with different surface tensions for the calculation of a wetting force measure of cleanliness [49, 50]. This test has many of the drawbacks of the water break test: the need for flat surfaces, the presence of surfactant, and the purity of the water used. In addition extreme care must be taken to maintain consistent experimental parameters like droplet size, humidity, and time before actual measurement.

Cohen *et al.* described a similar method for determining cleanliness based on surface tension measurements [51]. A series of liquids with surface tensions varying from 27 dyne/cm to 107 dyne/cm were dropped onto a cleaned surface. Using the criteria that a liquid with surface tension lower than the surface free energy would spread out on the surface, an



estimate of the surface free energy, hence the cleanliness, was obtained. This test is simpler than the contact angle test and requires no special equipment to be run.

In the residual pattern method [52], cleaned panels are dried for about 20 minutes at a temperature of around 120 °F. The presence of a stained area after drying indicates residual soil and inefficient cleaning.

The fluorescence method is very slow and less sensitive than the atomizer or water break tests. Panels are smeared with a fluorescent oil, cleaned and inspected under ultraviolet light. Visible fluorescence would indicate the presence of oil on the surface.

A variety of gravimetric tests are in use for evaluation of cleanness. In one method [53], the cleaned part is washed with ether. The weight of residue left on evaporation is used as a measure of solvent effectiveness. In a different test [54], panels are weighed to the desired accuracy and then smeared with oil or grease. After cleaning, the parts are rinsed and dried in an oven. The dry parts are placed in a dessicator and allowed to cool to room temperature. The parts are then reweighed and the difference in weight before and after cleaning is the residual contaminant. This test is sometimes used in conjunction with the black light fluorescence test where parts are exposed to black light in a dark room. Incomplete soil removal is detected by the presence of white fluorescence.

In the electronics industry, particulate contamination in the head/disk assembly (HDA) is evaluated using turbidity/liquid-particle-count (LPC) measurements [55]. Contaminant particles are extracted into an aqueous medium under ultrasonic action. The liquid is then subjected to turbidity measurements by passing light through it and measuring the

scattering from suspended particulates. Nagarajan [56] described a method for calculating surface cleanability by performing multiple ultrasonic extractions.

A more complicated method that has been used to determine cleanliness is the radioisotope tracer technique [57, 58]. Panels are uniformly coated with soil tagged with a radioactive element. The radioactivity is determined, and the panels are then subjected to various cleaning cycles. The radioactivity is measured again and the amount of remaining radioactivity indicates the amount of soil still present. While this is a very sensitive test, the use of radioactive materials creates certain practical difficulties. This is a time-taking exercise since radioactive soil has to be prepared each time. A Nuclear Regulatory Commission (NRC) license is required, and there is a need for special equipment and trained personnel. This method is probably best used when a specific invariant contaminant is desired to be removed.

McQueen and Allard [59] evaluated ultrasonic cleaning efficiency on-line by measuring the Galvani potential between two electrodes in an aqueous solution. When the current flow is very small, the potential between two electrodes in an electrically conducting medium is called the Galvani potential. Contamination levels of less than a monolayer can be detected, corresponding to a reading of a few millivolts. Electrochemically passive electrodes are required for this test, rendering it unsuitable for some common substrates like stainless steel and aluminum.

Razor blade edges are tested for cleanliness by determining the rate of evaporation from the surface of a test liquid containing a radiotracer element [60]. Thin metal coatings are applied to the blade edges and this

method of evaporative rate analysis (ERA) is directly related to the failure rate of the coatings.

Cibula *et al.* [61] used an electronic charge decay (ECD) test for the external aluminum surface of space shuttle fuel tanks. The surface is bonded to thermal protection materials with a primer that requires a very clean surface for proper adhesion. The ECD relates surface potential decay to cleanliness.

The auto industry has used surface carbon analysis as a tool for measuring contamination on automotive body sheet steel [62]. Surfaces that are not clean can lead to peeling of paint and corrosion problems. After cleaning, the surface carbon content is found by measuring the carbon dioxide formed on combustion. Total carbon analysis tests have the disadvantage of changing the nature of the sample [63].

Optically Stimulated Electron Emission (OSEE), or Photo Electron Emission (PEE), can detect contamination in the range of a few angstroms (Figure 3.1). Gillum and Jackson [64] used this technique to test the performance of a series of alternative solvents. A copper/nickel/tin alloy substrate is contaminated with machining oils for cleaning prior to plating. The surface is illuminated with ultraviolet light. A collector placed across an air gap detects the emitted electrons and displays the measured current as a voltage. Contaminants on the surface act as a resistance, causing a decrease in the observed signal. Comparison of the signal before and after cleaning gives an estimate of the contaminant removed. This technique has the advantage of being flexible, nondestructive and fast. It is portable and provides a quantitative measure without contact. It can detect residue in the approximate range 0.25 to 0.50 mg residue/ft<sup>2</sup>. Farella *et. al.* [65]



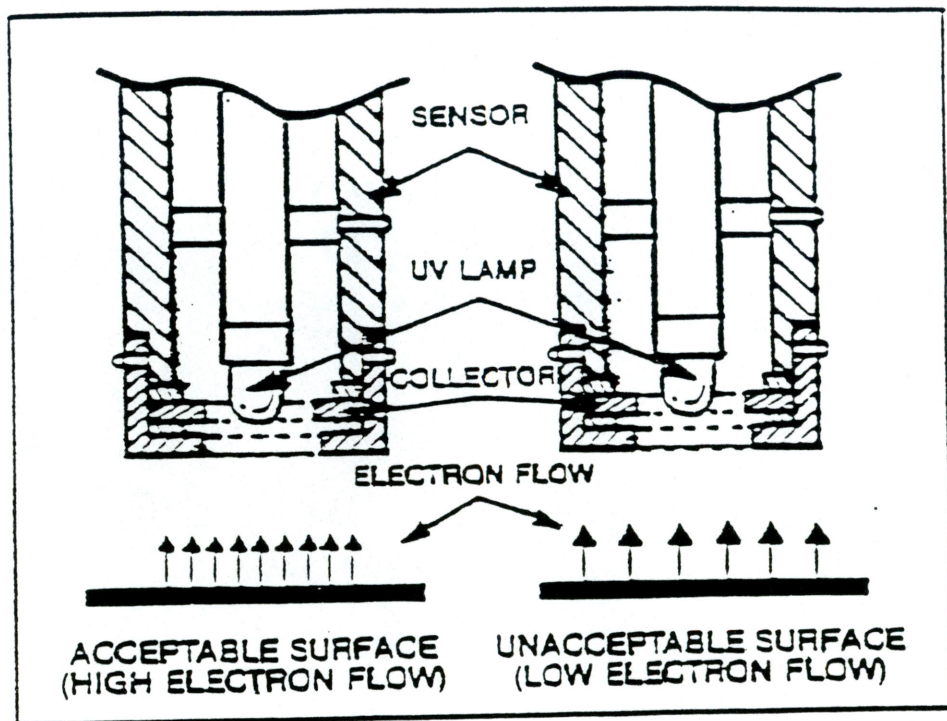


Figure 3.1 Schematic showing the principle of Optically Stimulated Electron Emission (OSEE) [64].



mentioned some of the disadvantages of this method of testing. It is not sensitive to the difference between oxide and grease, and fluorescent oils can interfere with the response. It also requires that a different calibration be prepared for each soil.

Leijon [66] used Electron Scanning for Chemical Analysis (ESCA) to analyze a 1010 cold rolled steel coupon. The analysis was performed as the part came out of the machine shop, again after polishing and then after vapor degreasing the coupon. XPS gives the elemental composition of the surface, and it was found that the amount of carbon decreased after these two operations. The coupon was then smeared with honing oil and then degreased again. The carbon, oxygen, and iron values were found to be very close to the original, indicating that all the honing oil had been removed.

Ray *et al.* evaluated defluxing in hybrid assembly cleaning operations using XPS. They found that the level of contamination was less than twice the escape depth of the photoelectrons, and the aluminum substrate was detectable. Contamination was artificially induced in known quantities to test the effectiveness of the cleaning solutions. The substrate was dipped in a 1 percent animal fat solution in isopropyl alcohol followed by a 0.25 M solution of sodium chloride. With subsequent cleaning steps, XPS analysis found that the levels of carbon,  $\text{Na}^+$  and  $\text{Cl}^-$  were reduced, and the aluminum substrate was more visible.

Farella *et al.* made XPS, contact angle and OSEE measurements on the same set of samples and found qualitative correlation between the respective results. An increase in contact angle and a decrease in OSEE signal was accompanied with an increase in XPS carbon signal. Similarly,

an increase in substrate iron signal was observed along with a decrease in contact angle and increase in OSEE signal. The apparent outliers present were attributed to the possible presence of cleaner or surfactant on the parts.

Thompson *et al.* [67] used XPS to quantify cleanliness levels for a variety of substrates contaminated with coolants and lubricants, cleaned with several different solvents. They chose a carbon-to-base-metal peak height ratio, called the "cleanliness ratio," as a measure of cleanliness. A low ratio was taken to be indicative of a clean surface, because it meant that more of the substrate metal was detectable through the layer of contaminant.

Powell *et al.* developed a barrel-ellipsoid diffuse reflectance FTIR instrument which was used for the analysis of stains on paper, metal, and other substrates [68]. Clean metal was used to take a reference spectrum. A drop of oil was then spread on the surface and vigorously scrubbed with tissue to reveal a visible stain. The resultant spectrum was sufficient to reveal that the oil was a vegetable oil. In a later study [69], contamination levels on machined metal surfaces were studied using 75° specular mid-infrared reflectance spectroscopy. Aluminum foil was found to be an adequate mirror for calibration and cleaning studies. The foil was weighed, wiped with oil, and weighed again. A calibration curve was prepared and it was used to predict contamination levels for a variety of substrates. Grazing angle spectroscopy was found to yield better measurements than diffuse reflectance for flat coupons.

Flux residues on printed circuit boards (PCBs) are analyzed using ultraviolet spectrography [70]. This method was adapted to study oil and

grease films on metal coupons at Dow Chemical Company [71]. A characteristic peak associated with the soil was identified, and a calibration curve was prepared to find the range of linearity. Cleaned coupons were extracted with a nonabsorbing solvent, and the ultraviolet absorbance of the extract was related to concentration of residue. This method assumes that the extraction solvent is capable of dissolving all of the remaining residue.

### 3.2 Review of Spectroscopic Methods

Various types of spectroscopic methods involving a range of special instrumentation, have been used for the detection of organic contamination on surfaces. Different techniques have been used to quantify or obtain qualitative information from the recorded data.

#### 3.2.1 XPS and Surface Analysis

The use of electron spectroscopies for surface analysis is now an established and expanding area. Both Auger and X-ray electron spectroscopies are capable of supplying information useful in the qualitative and semi-quantitative analysis of the near-surface region (top 1-100 Å) of solids [72]. The quantification of information obtained by these methods is an area that has been receiving more interest in the last few years [73, 74]. Thus far, sample matrix and instrumental problems have been considered too formidable for reliable quantitation.



Studies on quantitation have relied on simplifications like the assumption of homogeneity within the analysis depth and the use of ratios and percentages to express results. The difficulty in obtaining pure element standards is an important aspect which prevents absolute quantification. Other factors [75] which need to be known to the spectroscopist in order to obtain an absolute determination are : (1) The probability of ionization of the photoelectron must be available or estimable, (2) The electron transport processes in the solids which determine escape depth must be well described, and (3) The analyzer and detector efficiencies must be quantitatively described over the entire energy range of interest. Determinate error in these parameters can be expected, hence relative measurements are resorted to. Several studies have, however, used ESCA as a tool to detect contamination, often just taking the elemental composition as an indicator.

Wagner [76] used several sodium and fluorine containing samples and found that relative photoelectron intensities from chemically different species can show wide variations. Swingle [77] later showed with similar samples that surface contamination can have a drastic effect on measured elemental ratios when the differences in kinetic energy of the photoelectrons are large. The rate of intensity loss was found to depend on the vacuum level and the composition of the vacuum.

In the laser and electro-optics industry, cleanliness of components is often a vital issue. When surfaces are not clean, excessive scatter or absorption will lead to reduced performance, optical damage, or accelerated device failure. XPS was found to be a powerful technique for studying surface-related phenomena in a nondestructive way [78]. The processing



contaminants on polished lithium niobate crystals were examined using an XPS survey of a 600 micrometer spot over the 0-1100 eV binding energy range. Carbon, sodium, fluorine, potassium, phosphorus and chlorine contaminants were detected which were traced to cleaning and acid-etch steps during manufacture.

Ray, Artaki *et al.* [79] monitored the surface cleanliness of hybrid assemblies using XPS to determine if a mixture of CFC-113/Acetone has the ability to clean ionic as well as non-polar contamination species. Triple track gold conductors over ceramic substrates were tested at an average of two spots per sample, one spot on the conductors and one on the ceramic. It was shown that for dirty samples, the thickness of the contaminant coating was more than the escape depth of the photoelectrons, as evidenced by the almost negligible substrate aluminum peaks in the spectrum. It was found that clean samples had contamination from mishandling in the form of ionic species ( $\text{Cl}^-$  and  $\text{F}^-$ ). Fingerprints were also present, which were the cause of reliability problems under temperature cycling or temperature, humidity, bias (THB) testing of the samples.

The use of surface elemental compositions as determined using ESCA was shown to be comparable to OSEE measurements [80]. Analysis of 1010 cold rolled steel before and after cleaning yielded useful results, but it could not be determined whether the carbon present after cleaning was from the contaminant or cleaner.

### 3.2.2 Applications of Infrared spectroscopy

The development of infrared analytical methods has helped tremendously in the understanding of surface chemistry and has helped experimentalists monitor the composition, ordering, and oxidation states of species on surfaces. Infrared spectroscopy, once thought to have been hampered by its low sensitivity, has seen drastic improvements in instrumentation which have by and large overcome the problems produced by low-intensity IR sources and intrinsically inefficient IR detectors. The higher resolution has been accompanied by greater throughput, and the multiplex advantage of Fourier transform interferometry combined with powerful, computer-supported data acquisition and handling.

Diffuse reflectance infrared techniques have met with wide acceptance and can be used with powders, turbid liquids, and to some extent, with coatings on flat surfaces. Willey [81] was among the first to demonstrate the improvement in diffuse reflectance capabilities in the mid-infrared with the use of an integrating sphere. But this method was found to be inefficient, requiring a lot of time to obtain reasonably good spectra. Griffith and co-workers [82] and Krishnan *et al.* [83] used a diffuse reflectance accessory with ellipsoidal mirrors in conjunction with a commercial Fourier transform instrument, and showed this to be a powerful sampling method.

Diffuse reflectance has aided in the analysis of colors and identification of pigments [84]. The change in color of food materials and its significance in analysis has been demonstrated [85, 86]. The application

to paper and pulp material analysis finds extensive mention in the literature. Luner and Cohn discussed the role of reflectance methods in the control of whiteness and brightness of wood pulp during the paper making process [87]. Vaeck [88] showed that a touch of blue suggests a higher quality of white while any other hue would be taken as an indication of lower quality. This principle was subsequently found to be of equal validity in the textile industry [89].

In the near-infrared, diffuse reflectance is a very important tool in the quantitative investigation of substances adsorbed on a solid surface. Sample preparation is a crucial part of this examination, and the particle size of the adsorbent has been shown to have considerable influence on the reflectance spectra [90]. The nature of the sample surface also affects the spectra, and surfaces with little or no gloss were found to yield better results. Other applications in the infrared include experimentation at different temperatures, analysis of amino acids, and pharmaceuticals [91].

Powell *et al.* developed a barrel ellipsoid diffuse reflectance accessory for a portable surface inspection instrument and used it in the study of paper type, effect of light on paper, and the detection of vegetable oil stains on machined metal surfaces [92]. The sensitivity of this method was found to be less with very flat metal surfaces.

In recent decades, external reflection spectroscopy has found increasing use in the probing of bonding at metal surfaces and coatings on rigid metal plates. Both single and multiple reflection techniques were used and Greenler [93] showed that for a single reflection the optimum angle is around  $88^\circ$ . For multiple external reflection, Greenler showed that there is a specific number of reflections for maximum band intensity. At



grazing angles, the standing wave formed by the incident and reflected rays at has a large amplitude and good quality spectra can be obtained [94, 95]. This led to the technique being used in the study of monolayers, coatings, and corrosion products on metal surfaces.

Handke *et al.* and Ishitani *et al.* [96, 97] studied the spectra of thin layers of grease and organic coatings on metals. Wooton and Hughes [98] applied external reflection infrared spectroscopy to the study of lubricants. Engine parts with contamination in the form of varnish, carbonaceous deposits, and corrosion were tested before and after cleaning with pentane. Grazing angle reflectance measurements were taken and both visible and invisible contaminants were detected. The visibility of these materials was related to the thickness of the surface deposit. Various degrees of oil oxidation on the parts was identified. Specular reflection spectra of various vegetable oils on a galvanized steel coupon collected by Powell *et al.* [99] are shown in Figure 3.2.

Smith *et al.* [100] examined the composition of several blended gasolines using FTIR spectroscopy. The composition and its effect on the properties which determine the octane number was studied. Gasoline of 87 octane, 89 octane, and 93 octane were obtained from several standard pump stations. The relative ratio of methyl to methylene groups, hence the degree of alkane branching, was determined. As expected, the methyl/methylene ratio showed a continuous increase from 87 to 93 octane.

A monolayer of arachidic acid on a silver substrate was examined using external reflection methods by Schlotter *et al.* [101]. Information about the bonding between substrate and adsorbate and the orientation and packing density of the alkyl chains was obtained. External infrared



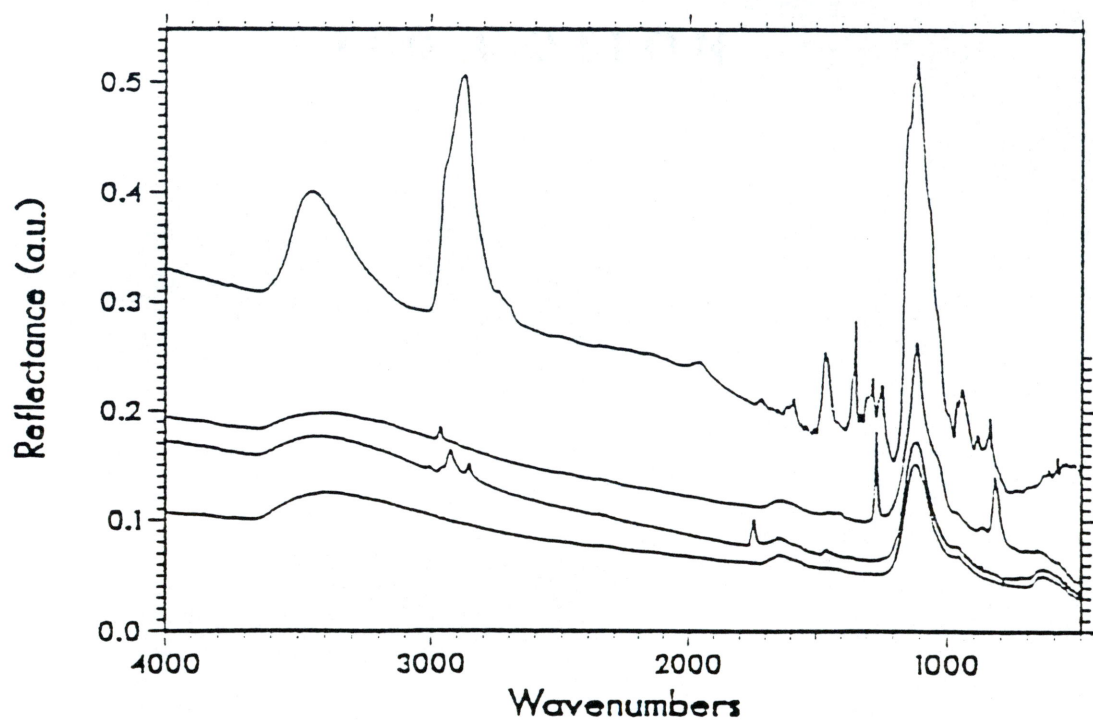


Figure 3.2 Specular reflectance spectra of contamination on galvanized metal sheet (from bottom to top): unstained, corn oil, silicone oil, and orange ink [99].

techniques have found applications in the characterization of monolayer films, films on glassy carbon, and polymer films, among others [102].

### 3.2.3 Ultraviolet Region

Ultraviolet spectroscopy has been used with a fair degree of success in the monitoring of oil contamination. Many auxiliary lubricants used on hot aluminum-rolling mills are based on high viscosity mineral oils containing aromatic hydrocarbons which fluoresce upon irradiation with ultraviolet light. Mineral oils from various geographic locations and processing streams have different UV-absorption and emission characteristics. This property has been used in the identification of oils and detection of sources of hydrocarbon contamination in the environment [103]. UV-fluorescence spectroscopy has been used in the study of emulsion-type lubricants to detect tramp oil contamination [104]. The presence of mist lubricant, the most common source of contamination, was monitored using UV-fluorescence spectroscopy. Different concentrations of emulsion lube were used for the experiment, and the intensity of fluorescence emission was measured. This intensity was found to increase with increasing concentration of contaminants. The method was found to be simple and effective for semi-quantitative measurements.

The very purpose of cleaning parts is defeated if the solvents in use are in themselves contaminated. This problem has been addressed by E.B. Murphy [105] using an ultraviolet reflection method. In these tests, quartz paper and cloth coupons, which typically reflect 70-90 percent of the light on solvent-immersion and subsequent drying, were used. The sensitivity

was found to be greater with paper because of the higher density of fibers in its structure. In the first set of tests, reflection of clean paper was compared against reflection from paper dipped in 1,1,1 trichloroethane (1,1,1 TCE) contained in the cold-immersion tank of a degreaser and paper dipped in 1,1,1 TCE taken from a drum. This led to the conclusion that it is best to process the parts through the vapor-distilling section of the degreaser last, as opposed to the cold-tank section, because there is a greater chance of contamination there. The next set of tests was performed using three alcohols: methanol, ethanol, and propanol. Contamination was found again in these cases which was accidental, or in the form of ingredient antioxidants. This method was demonstrated to be one of qualitative significance for non-volatile residue (NVR) detection.

Archer et. al. [106] applied ultraviolet spectrography to the determination of rosin residues on cleaned electronic assemblies. The characteristic absorption peak of abietic acid, a major rosin component, was chosen as the basis for the method. Abietic acid has a major absorption peak at 241 nm (Figure 3.3). Calibration curves of micrograms of abietic acid vs. absorption were prepared down to concentrations of 1-2 mg rosin/in<sup>2</sup>. Sample circuit boards were precleaned in a solution of 75 percent volume isopropanol and 25 percent volume water, and dried prior to fluxing and soldering. The boards were then sprayed with a flux, soldered, and cleaned in an open top vapor degreaser. The assembly was then placed in a bag and shaken in American Chemical Society (ACS) grade isopropanol for five minutes. A background spectrum of the solvent was obtained using ACS isopropanol, and then a spectrum of the rosin in isopropanol was taken. The resultant spectrum showed the characteristic

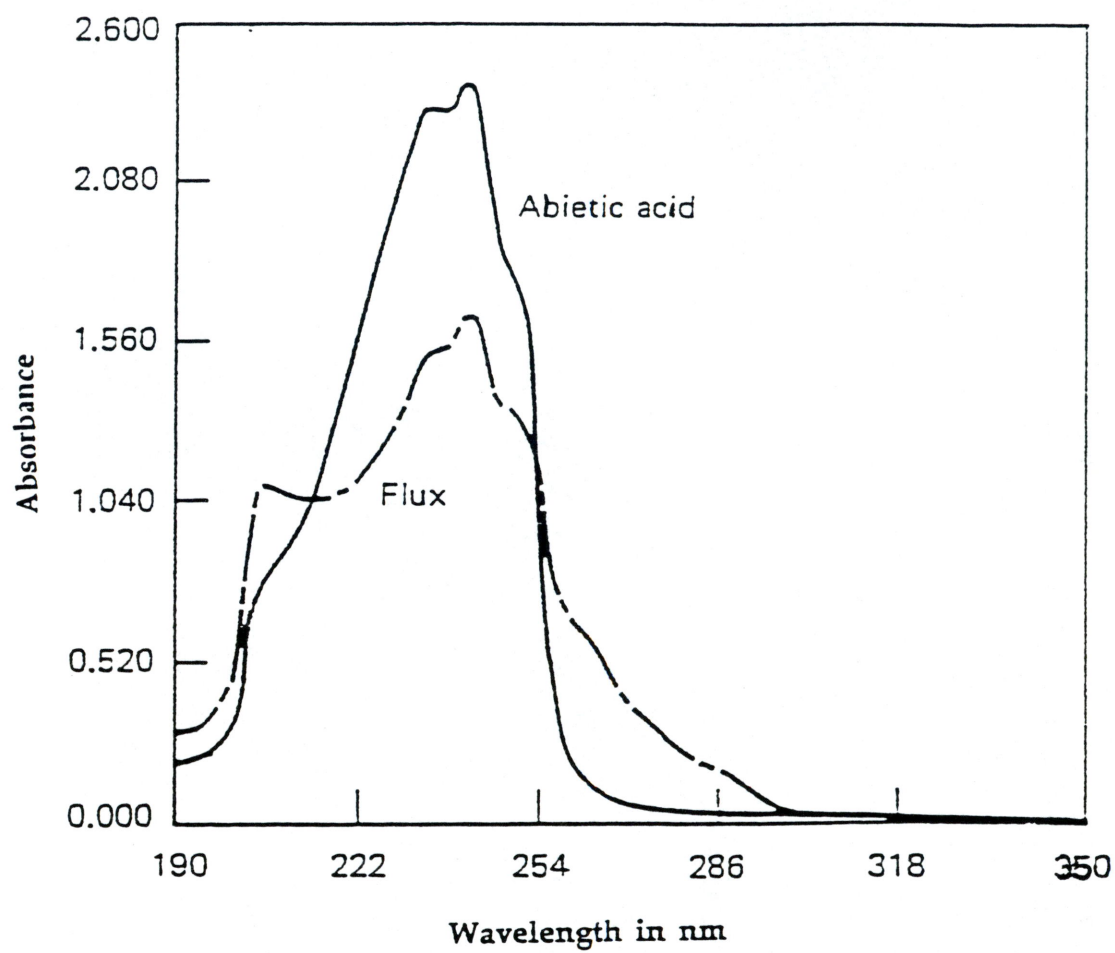


Figure 3.3 Ultraviolet spectra for abietic acid and a rosin flux [105].



abietic acid absorption at 241 nm. The concentration of rosin was then calculated by comparison with the calibration curve. Cleaning cycles involving different cleaning times and solvent combinations were performed, and the results compared using this method.

Reflectance measurements are often required to obtain reasonable data for contamination analysis purposes. Unlike transmission spectrophotometry, diffuse reflectance spectrophotometry usually results only in relative measurements. Since no perfect diffuse reflector (with a reflectivity of unity) is available, investigators must use reference standards with high reflectivities, and reference measurements to these standards. While special and complicated methods exist to measure the absolute reflectance of the standards themselves, Gillespie and Lindberg [107] sought to design a simple method allowing nearly any instrument to make these measurements. Careful sample preparation is entailed in following this procedure.

## 4. EXPERIMENTAL METHODS

The samples for this thesis were various dirty metal parts with different contaminants taken from processing operations in industries. These parts were subjected to cleaning with different alternative chemistries, and analyzed for remaining residue using different techniques. In the sections below, the stages in the cleaning process, sample handling and preparation for testing, and surface analysis steps are explained in detail.

### 4.1 Decontamination of parts

Six representative alternative chemistries were available for testing in the laboratory. These cleaners, chosen to cover the broad range of classifications are: (1) n-methyl pyrrolidone (NMP), (2) terpene with d-limonene (TE), (3) hydrocarbon (HC), (4) aqueous alkaline (AL), (5) aqueous acidic (AC), and (6) dibasic esters (DBE).

For parts cleaning, a system consisting of an ultrasonic tank, two rinse tanks and a hot air convection dryer, was used. The parts used in the experiments were sufficiently small that they could be placed in a large beaker (800 ml.). To conserve cleaner, the ultrasonic tank was filled with water, into which was immersed an appropriately clasped glass beaker containing the cleaner and dirty parts.

From the literature [108] it was determined that time of cleaning, temperature of the bath, frequency of the waves, and cleaner composition are important factors in ultrasonic cleaning. It was hence decided to vary

these factors, and see the response on cleaning efficiency. The concentration was not considered a variable for the experiments carried out because undiluted use was recommended for most of the cleaners. Runs were performed at different conditions of time, temperature and ultrasonic frequency for each of the solvents.

A  $2^k$  factorial statistical model was used to determine the parameters affecting the experiments [109]. This required the determination of a higher and a lower value for each of the operating variables, for each solvent. The choice of these values was based on cleaner material safety data sheets (MSDS) information that detailed precautions to be taken, and manufacturers recommended values [110]. Temperature was varied from a high of about 20 °F below the flash point to a low of about 20 F below the high, as long as the low was not below room temperature. Time of cleaning was varied from one to five minutes. Ultrasonic power was changed from 200 W to 350 W, covering the operating range of the tank. Cleaning was done at the eight possible combination conditions of these extreme values and at the mid-point of these values. This was done to ensure that the parts were subjected to the entire possible range of operating conditions.

Contaminated parts used in various stages of manufacturing were received along with a filled-out questionnaire listing the processes they had undergone, and a sample of the contaminant. The Solvent Alternatives Guide (SAGE), developed for the EPA, is a software that allows users to make decisions regarding the choice of chemistry and process for the parts in hand [111]. Inputted into this system are the results of several tests conducted over the years. This database was taken as a



reference point for experiments carried out. For each set of parts, the SAGE program was run to determine the recommended choices. Results obtained were later compared with SAGE predictions for database enhancement purposes.

During the cleaning stage, dirty parts were placed in a beaker containing the cleaner, which was then lowered into an ultrasonic bath containing water. The alkaline cleaners were used at 25% concentration, and the other cleaners were used undiluted. After cleaning for a time period according to the factorial chart, the parts were removed from the beaker using clean tongs, allowed to drain free of solvent for a few seconds, and placed in a perforated metal basket. The rinse tanks, of which the baskets are a part, consist of a rotating basket assembly and a turbo-charger to provide agitation in the tank. The parts were rinsed for three minutes in warm, distilled water by the rotation-agitation process and then taken to a drying unit. Two rinse stages were used to endure the removal of any solvent that might be left on the parts from the cleaning step. The hot air convection dryer was equipped with the same basket-rotation device and was operated at 185 °F for four minutes or until the parts were completely dry. Dry parts were sealed in glass bottles to avoid re-contamination prior to testing. This process was repeated for each cleaner, for each condition. Used cleaner was disposed of according to previously classified groups of hazardous waste or non-hazardous waste, as determined from information supplied by the manufacturer.



## 4.2 Cleanliness testing using ESCA

Clean and dirty parts were analyzed using Perkin-Elmer instrumentation with an aluminum anode [112]. Since this method depends on the presence of a strong vacuum, very dirty parts coated with large amounts of oil were not used. Instead, relatively unsoiled parts with less visible oil were used to obtain data on dirty parts. Parts taken from the glass jars were placed on a round sampling plate that was then introduced into the vacuum chamber on a platen driver. When the pressure was down to the desired level, the plate was pushed into the analysis chamber. Once the sample plate was in position, the spectrometer was programmed to analyze each part at three different spots of 0.8 mm diameter. The data acquisition time was set at ten minutes for each spot. Data was obtained for dirty parts, parts cleaned in the laboratory, and parts cleaned by the companies using their current CFC-based process. In order to determine more accurately the actual composition the base material without any contamination present, sputter-cleaning of the part was done. An ion-gun was trained on the part and sputtering was done for five minutes during which the thin contaminant layer was destroyed so that the bare metal was visible to the spectrometer. A video camera attached to the spectrometer allowed for continuous monitoring during the scanning stage, and for selection of spots on the part where scans were to be taken.

Once the data was recorded, it was displayed on an accessory computer terminal in the form of an elemental spectrum. The peaks in the spectra were identified using an in-built identification program and ESCA line position tables for aluminum  $K\alpha$  X-rays. The data was

smoothed, and artifacts as tiny peaks at the base of each spectrum peak were satellite subtracted.

#### 4.3 Cleanliness testing using Infrared

Both diffuse reflectance and external reflectance spectroscopic methods were tried, to determine the level of cleanliness. Both methods required the selection of a proper background and reference standards.

Diffuse reflection tests were carried out using a spectrometer system developed by scientists at ORNL. The portable surface inspection instrument, Inspector<sup>TM</sup>, consists of a barrel ellipsoid diffuse reflectance sampling terminal, which is attached to a small, light MIDAC 2501-1 illuminator<sup>TM</sup> (20 cm by 20 cm by 60 cm, 13 kg). This system was developed to assist in the analysis of remote samples with a large flat or convex surfaces at different points.

For specular reflection measurements, a Bio-Rad<sup>®</sup> instrument available at ORNL was used. The sample preparation methods used were the same for both techniques.

For obtaining reference spectra, gold mirrors were used. These mirrors were front-surfaced, and of high quality. Before taking reference spectra, it was necessary to make sure that the reference mirrors were adequately clean. To ensure this, the mirrors were degreased with a pine-oil based cleaner, followed by a 1-ks soak in concentrated sulfuric acid. The use of sulfuric acid was to make sure that none of the cleaner remained on the mirror after the wash. The mirror was then thoroughly rinsed with distilled water, and dried rapidly in a nitrogen stream.

In order to view spectra from the oils on the parts without artifacts from the metal substrate it was necessary to have a background reference of a perfectly clean metal whose contribution could then be subtracted from the spectra obtained. Since this clean metal was to be compared with other samples cleaned using alternative cleaners, it was a necessary requirement that the reference sample be of a higher order of cleanliness. A procedure similar to that used for the background gold mirrors was applied to achieve this objective. The metal sample was first cleaned with a regular detergent, followed by a distilled-water rinse. It was then washed in very dilute sulfuric acid and rinsed again with distilled water. Finally, it was blow-dried in a stream of argon.

In order to obtain quantitative information from the data taken, a calibration curve was prepared [113] using multivariate techniques. Metal samples cleaned as described above, were weighed using a sensitive balance with recording capability of upto five significant digits. The coupons were then smeared with a drop of contaminant, which was evenly spread over using a tissue paper until none of the oil was visible. The part was weighed again to determine the weight of applied contaminant. This process was repeated for varying amounts of contaminant until data points were obtained for different levels of contamination of parts. Included in the calibration data set were coupons that were weighed, contaminated, cleaned, and re-weighed again.



#### 4.4 Cleanliness testing using Ultraviolet

Ultraviolet spectroscopy was used to characterize the cleanliness of metal coupons with contaminants having absorbance in the ultraviolet region. A fiber-optic SD-1000® dual spectrometer was used for making the measurements (Figure 4.1).

The assembly consists primarily of a fiber optic spectrometer with a wavelength range of 225 nm to 350 nm and uses a 1024 element charge coupled device (CCD) detector. The spectrometer has two components, a master and a slave. This setup allows for making corrections for changes in the lamp without taking a new reference. The slave spectrometer receives the light directly from the source. The master receives light reflected from the sample surface. A seven fiber reflection probe is used to direct light from the source onto the sample, and to collect reflected light. The probe consists of a silica UV quality central transmission fiber surrounded by six similar receiving fibers. The light source for the instrument is provided by a high pressure pulsed xenon source through an SMA connector. An analog-to-digital (AD) board compatible with a personal computer was used for data acquisition. Minimum loss, single-strand, bifurcated fiber optic cables of 200 micron core diameter, and length over two meters were used for light path.

Clean metal samples for reference measurements were prepared in the same manner as for infrared measurements. Before the source was turned on, a dark measurement was taken with the light off. This was done to ensure that the contribution from any stray light entering the system could be subtracted later. The light was then turned on, and a



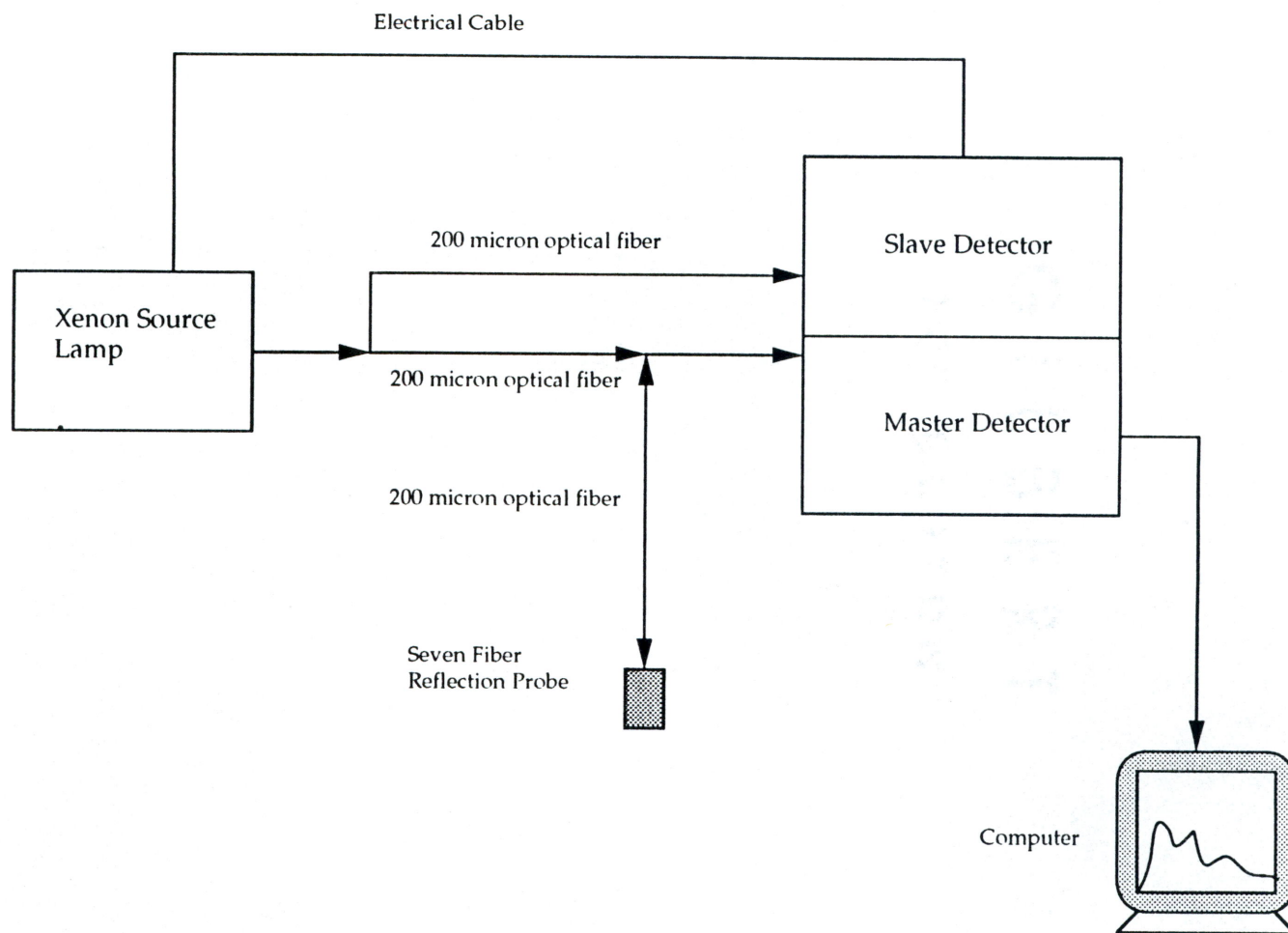


Figure 4.1 Ultraviolet Fiber Optic Spectrophotometer

reference measurement was taken of the clean metal sample. Absorption off the oil on a contaminated metal sample was then measured.

The SpectraScope software accompanying the SD-1000 instrument was used to modify parameters in order to get better data. The analog to digital (ADC) data sampling frequency, which sets the exposure time for the CCD, was adjusted for each experiment to maximize the detector output voltage and signal to noise ratio. The input gain on the ADC device changed as necessary for amplification. A long integration time was set for the CCD and a high number of scans were taken and averaged for consistency. In order to smooth the data, a moving average of adjacent pixels was applied to the data array. For the 200 micron fibers in use, option 17 was chosen which averaged eight pixels on either side of each pixel. The light source was set up to provide a continuous stream of pulses during the scan period. The absorbance drift correction option was chosen to allow for changes in light levels detected by the slave to be subtracted from the master, hence compensating for drift in the light source.

#### **4.5 Cleanliness testing by gravimetric analysis**

Quantitative testing for particulates and organic residue on the cleaned parts was performed using the testing procedure as outlined in MIL-STD-1246B [114] for non-volatile residue (NVR). The setup of apparatus for this experiment is shown in Figure 4.2. The samples were placed in an appropriately sized beaker, and 2-propanol was added until the part was totally covered. The beaker was placed in a small ultrasonicating unit for approximately three minutes. The beaker was then removed and

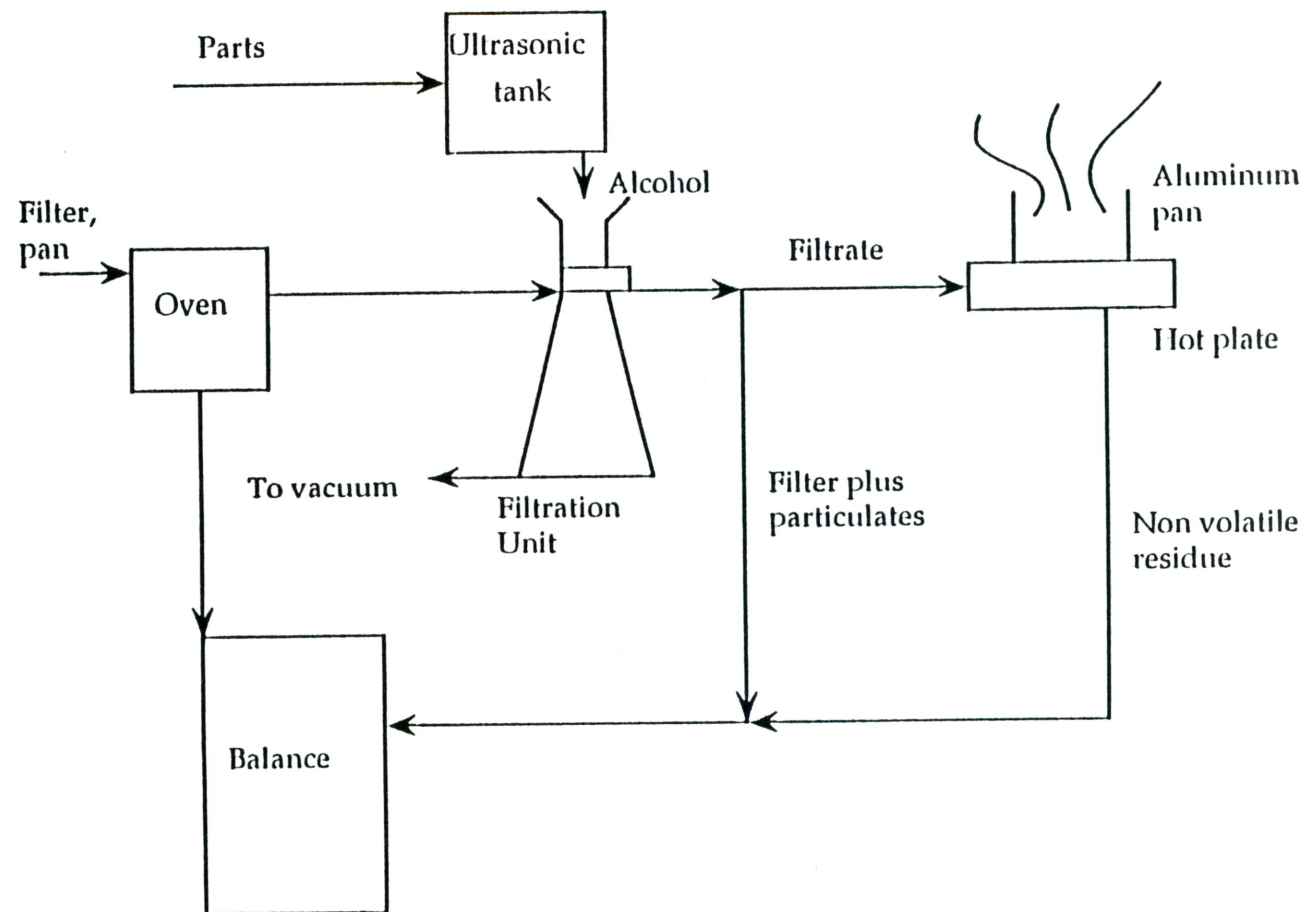


Figure 4.2 Apparatus for determination of particulates and NVR.

the parts taken out from it, after rinsing with 2-propanol to ensure that no residue had settled on the surface. Finely sieved filters were placed in a drying oven and allowed to dry for fifteen minutes. A filter was then taken out and weighed on a sensitive balance capable of measuring up to ten micrograms. The filters were placed in the oven and allowed to dry for a further ten minutes. They were then removed and reweighed. If the new recording was within 0.0001 gm of the earlier value, it was considered for use. If not, it was further dried until the criterion was met. The clean, dry filter was placed in the testing apparatus, making sure that the filter flask and beaker were tightly clamped. The solvent remaining from the cleaning of the part was then poured into the beaker and allowed to filter through into the flask. The vacuum pump was turned on to aid the filtration process. As the level in the beaker went down, it was washed with more propanol to make sure that no matter had adhered to the walls. Once filtration was complete, the pump was turned off and the filter carefully transferred to the drying oven. It was allowed to dry for ten minutes, after which it was cooled in a dessicator for five minutes. The weight was then recorded, followed by drying until a constant weight was obtained. The difference between this reading and that of the earlier one was taken to be the amount of particulate matter present on the part.

This procedure was followed by testing for NVR present on the part. A small, clean aluminum dish was pre-weighed. The solvent left in the filter flask after filtration was transferred into a beaker, adding propanol to rinse out the last of the contents. This beaker was placed on a hot plate under a hood and the solvent was allowed to evaporate. When the volume of the solvent became small, it was poured into the aluminum



pan. The contents of the pan were allowed to boil off until the organic residue left just started to oxidize or smoke. The pan was removed from the hot plate at this point and allowed to cool in a dessicator. The cool pan was then weighed, and the difference in weight from the empty pan gave the amount of NVR on the part.

The dimensions of the part were noted and the surface area was calculated in order to be able to express the results from the test in terms of weight of contaminant per unit surface area. The weight of the particulates and NVR were added to get the level of total contamination on the part. The above procedure was also done for dirty parts, company-provided clean parts, and laboratory-cleaned parts.

## 5. RESULTS AND DISCUSSION

### 5.1 Results from ESCA

Samples cleaned with various chemistries, under different experimental conditions, were analyzed using ESCA. Figure 5.1 shows the ESCA spectrum obtained from the surface of a copper switch used in electronic assemblies (Part MC1), covered with a contaminant layer consisting of cutting and drawing oils. This part was analyzed as obtained from the company before it was cleaned and sent for assembly into a larger product. A strong primary carbon peak is visible at 287 eV. The presence of oxygen in the contaminant is detected by the oxygen peak at 531 eV. The level of dirt present on the part is so high that the base metal, copper, is not visible on the dirty part spectrum. The level of carbon seen is taken to be indicative of the amount of contamination present on the part, since the contaminants are composed of hydrocarbons of which carbon is a principal constituent. The high level of carbon in this figure indicates a very dirty part.

Figure 5.2 shows the spectrum obtained from a similar part (Part MC11) after it had been cleaned with DBE. The carbon peak is noticeably much smaller in comparison to Fig. 5.1. The presence of copper is detected by the sharp peak at 934 eV. Secondary or Auger peaks for copper at 570 eV and 629 eV confirm its presence. This shows that the cleaner has removed a substantial amount of the contaminant from the surface. In Figure 5.3 the spectrum obtained from a part cleaned by the company using TCE, is shown. A comparative look at figures 5.2 and 5.3 shows qualitatively that

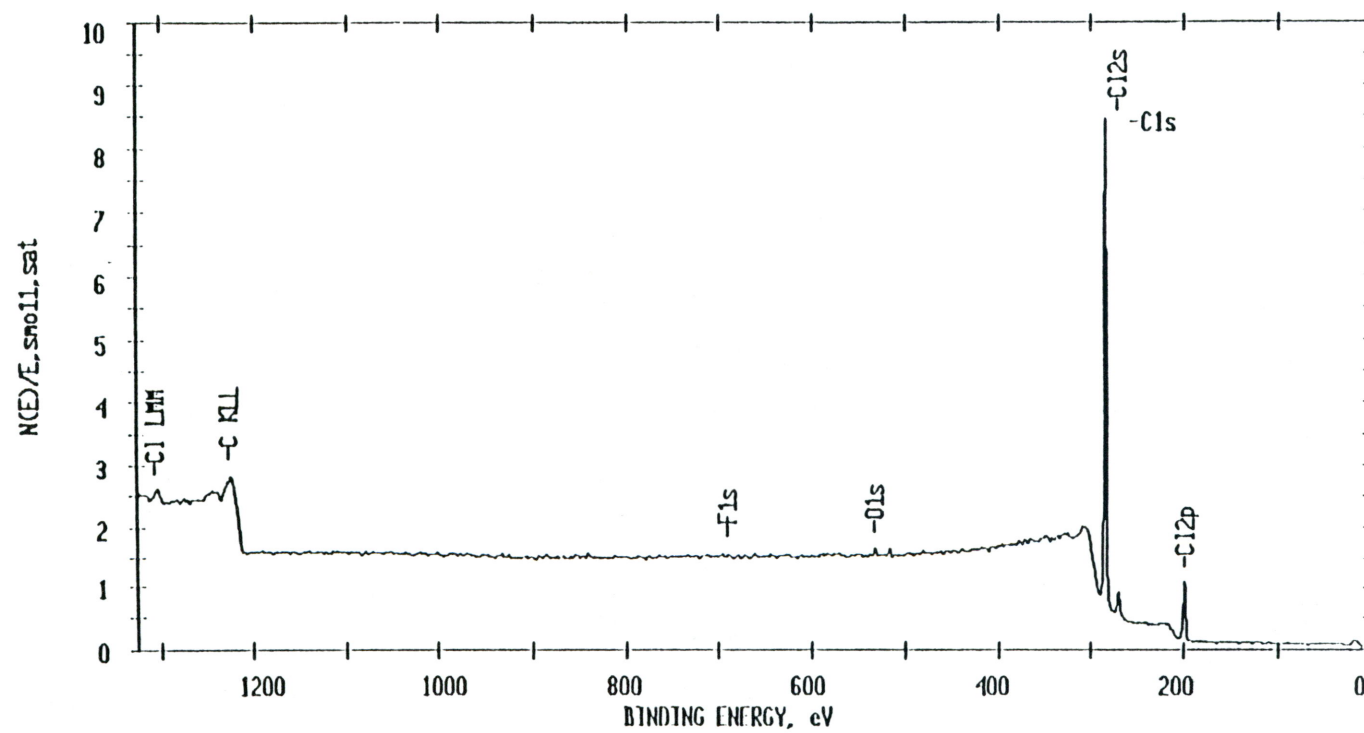


Figure 5.1 ESCA spectrum for copper switch contaminated with cutting oils.

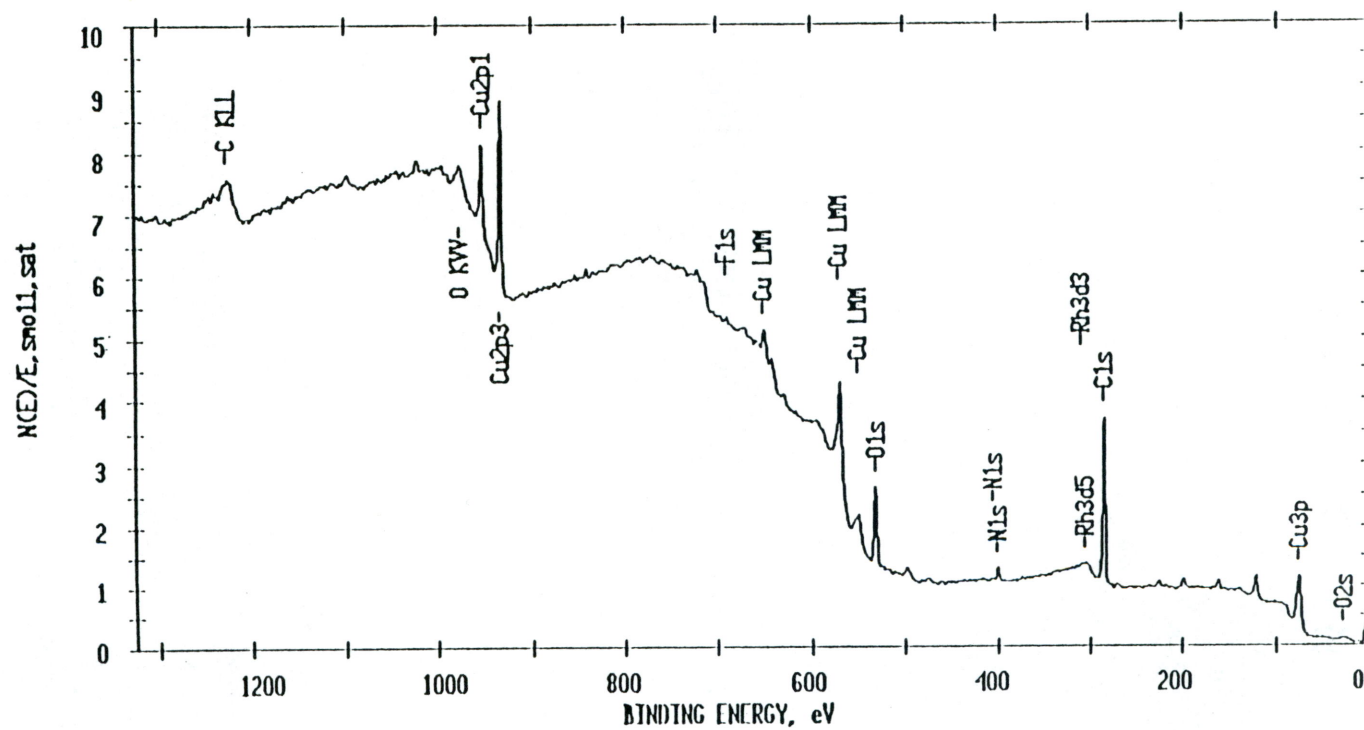


Figure 5.2 ESCA spectrum for copper switch cleaned with dibasic ester (DBE).



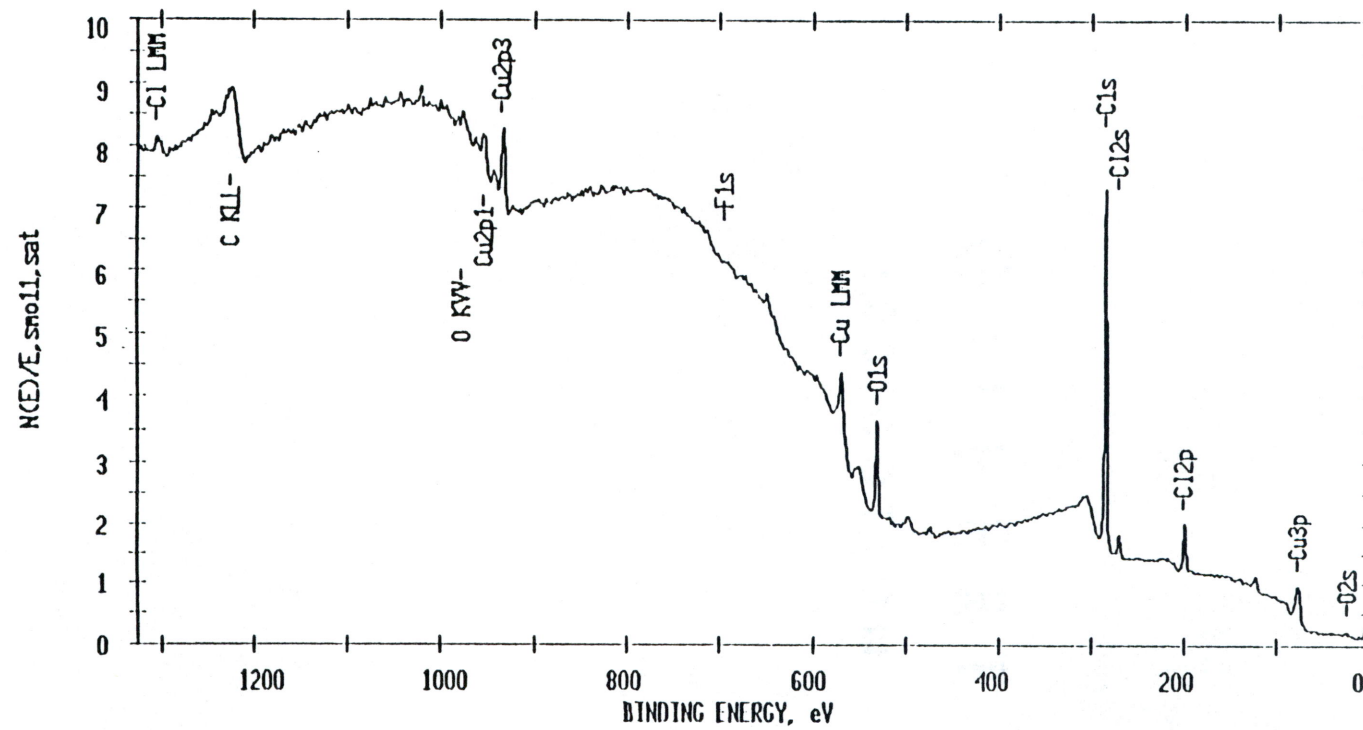


Figure 5.3 ESCA spectrum for copper switch cleaned by company with TCA.

the performance of the alternative cleaner, HC, is quite better, and suggests a possible alternative to the banned chemical from a cleanliness standpoint alone. In Figure 5.4 is shown the results of analysis of a 0.8 mm diameter spot on a similar part using the sputter technique for a period of fifteen minutes. Since in this case the X-rays have penetrated into the surface, through most of the oxide film on the part it is seen that the presence of carbon is almost negligible. The copper peak is the lone very strong peak, and it shows that the base metal consists mostly of this element.

Figure 5.5 shows the results from the cleaning of nickel heating coil (Part PTC) using two different cleaners, AL and NMP. It can be seen that the part cleaned with AL shows a lower level of carbon. Figure 5.6 shows comparative ESCA plots from cleaning the same part with different values of the experimental variables. This time, NMP gives the better results. This shows that it is necessary to optimize the conditions for each cleaner in order to obtain best results.

These parts were cleaned with six different cleaners at all experimental conditions as dictated by the factorial chart (51). Each part was then analyzed at three points on the surface using ESCA. Averaged carbon-to-nickel ratio results for cleaner AC at the nine conditions are shown in Table 5.1. The results of the experiment in terms of the effect of each parameter on the cleaning process is explained in detail in a thesis by Stafford [110]. The peak cleaning conditions for each chemistry are also identified in that work.

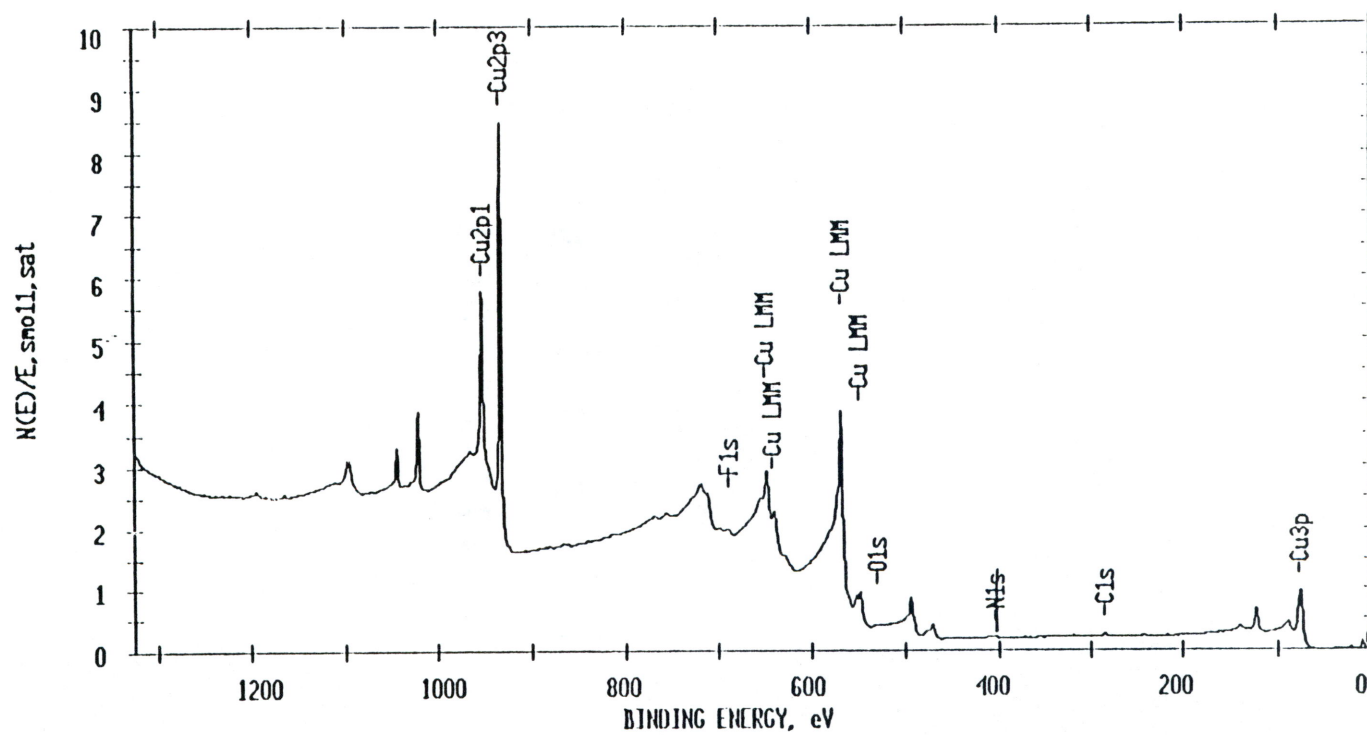


Figure 5.4 ESCA spectrum for sputtered copper switch showing base metal composition

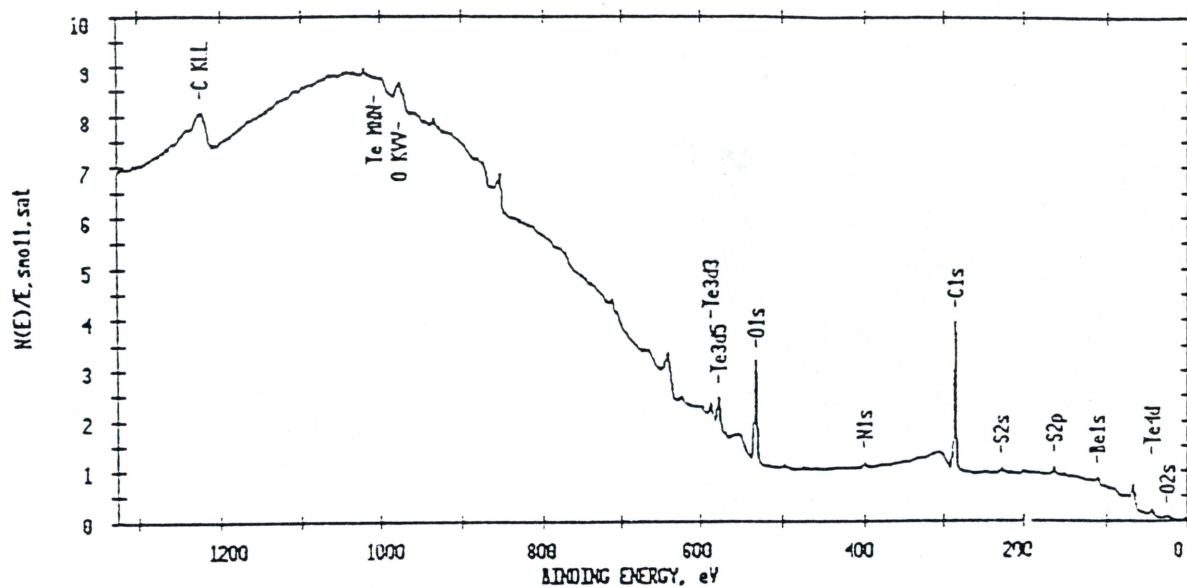


Figure 5.5 (a) ESCA spectrum for heating coil with an aqueous alkaline cleaner

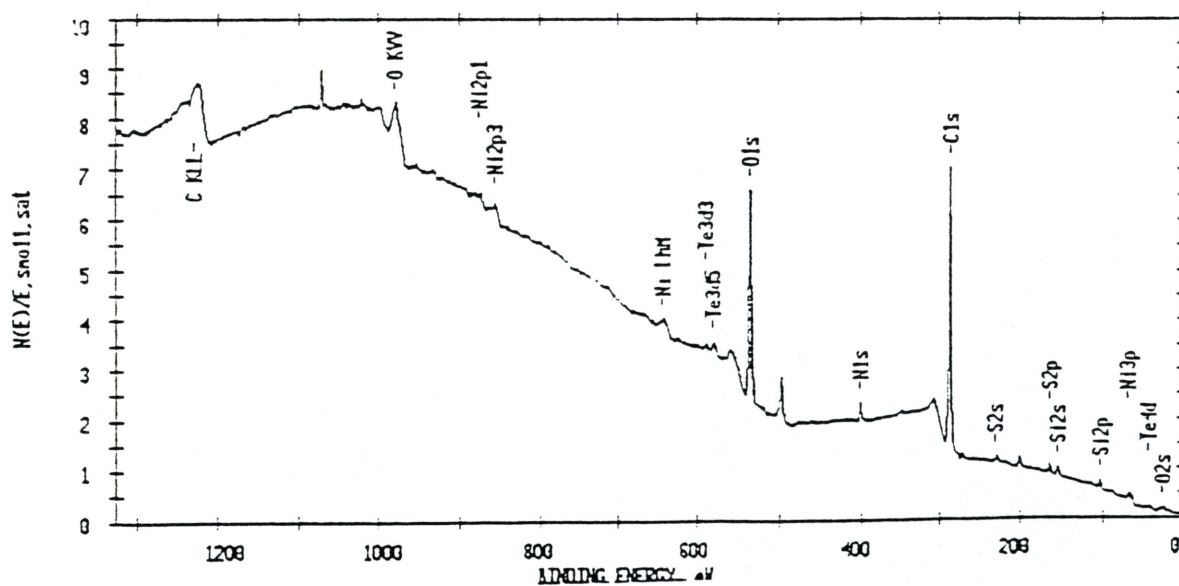


Figure 5.5 (b) ESCA spectrum for heating coil cleaned with n-methyl pyrrolidone



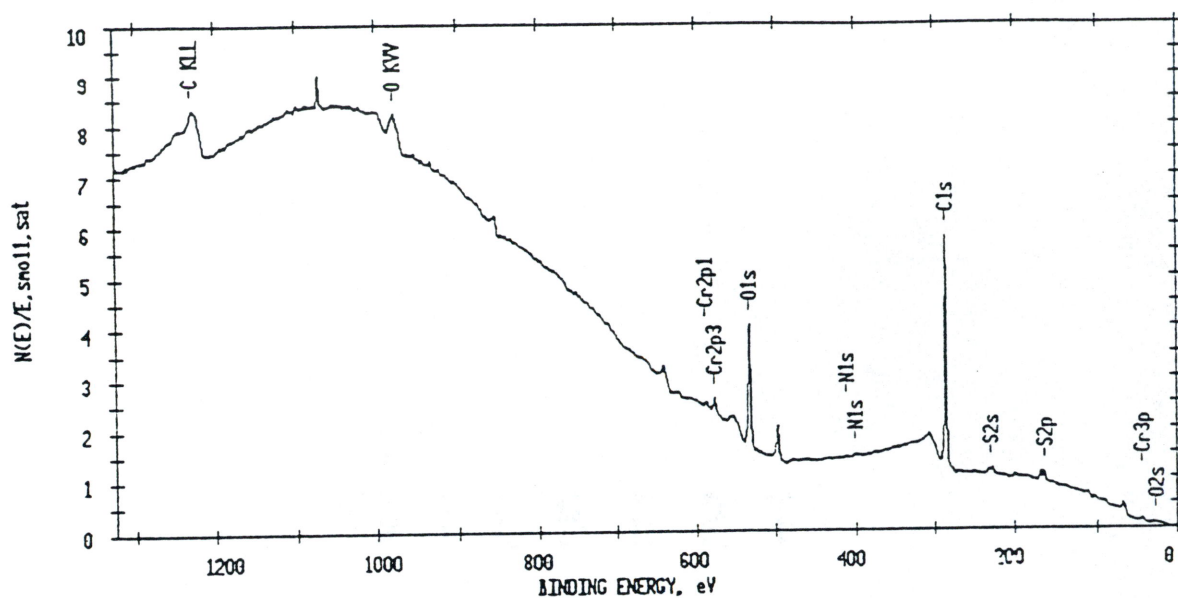


Figure 5.6 (a) ESCA spectrum for heating coil with AL at new condition, R2

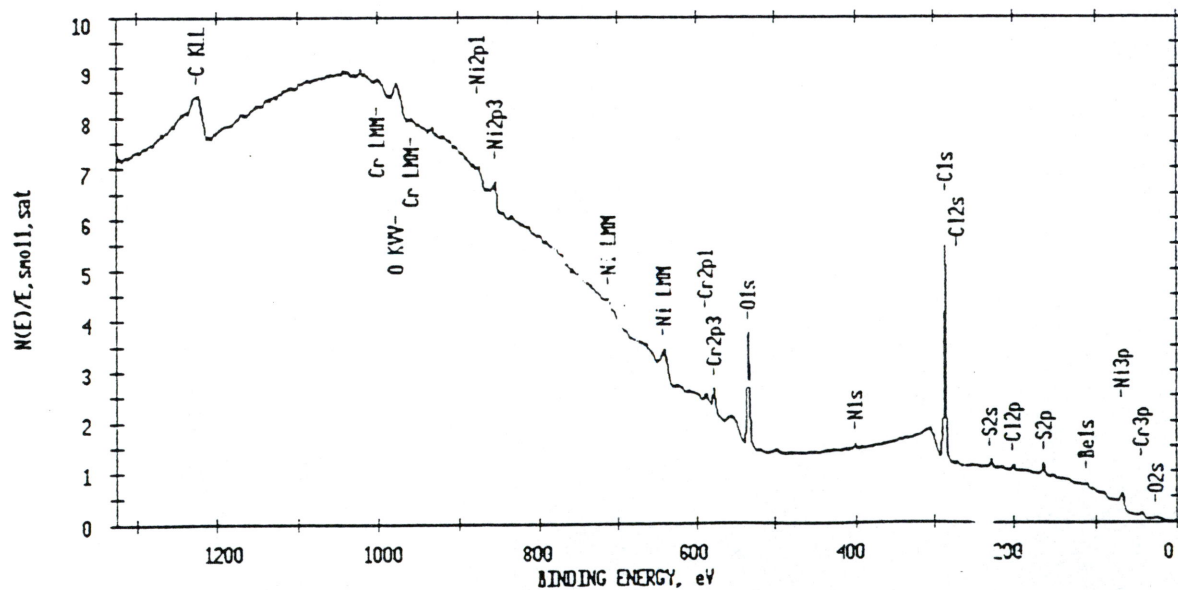


Figure 5.6 (b) ESCA spectrum for heating coil cleaned with NMP at new condition, R2

Table 5.1 Carbon-to-Nickel ratios from ESCA analysis of nickel heating coils at factorial conditions.

Run number	Ultrasonic Power(Watts)	Time (min)	Temperature (C)	Avg. C/Ni ratio
1	200	1	40	1.89
2	350	1	40	1.06
3	200	5	40	0.56
4	350	5	40	0.8
5	200	1	60	1.62
6	350	1	60	0.78
7	200	5	60	0.96
8	350	5	60	0.68
9	275	3	50	1.07

## 5.2 Results from Infrared Spectroscopy

Specular reflectance mid-infrared experiments carried out using a Bio Rad™ instrument available at the Oak Ridge Y-12 plant, were used to estimate the amount of contamination on parts. Figure 5.7 shows the spectra obtained from the cleaning of stainless steel coupons originally contaminated with cutting oils. These coupons were cleaned with the various cleaners available in the laboratory, and then tested for residual contamination against a background gold mirror. The spectrum lines are very flat, indicating that the parts are extremely clean. The upward slope of the lines is due to the reflection from the base steel, which was not accounted for in taking this data. A reference spectrum of a clean steel coupon was later made using the same gold mirror background, and this spectrum was subtracted from the rest to obtain a more horizontal series of spectra.

Infrared absorbance curves for steel parts with different amounts of contamination on the surface are shown in Figure 5.8. A gradual increase in peak height can be seen with increase in the level of contamination from bottom to top. Each coupon was weighed, contaminated, cleaned, tested, and reweighed again. Based on this series of curves a calibration set was created, relating infrared spectra to the physical amount of contaminant present on the part. The next plot (Figure 5.9) shows absorbance curves for parts made of two different types of steel, with the same contaminant, a cutting oil, on the surface.

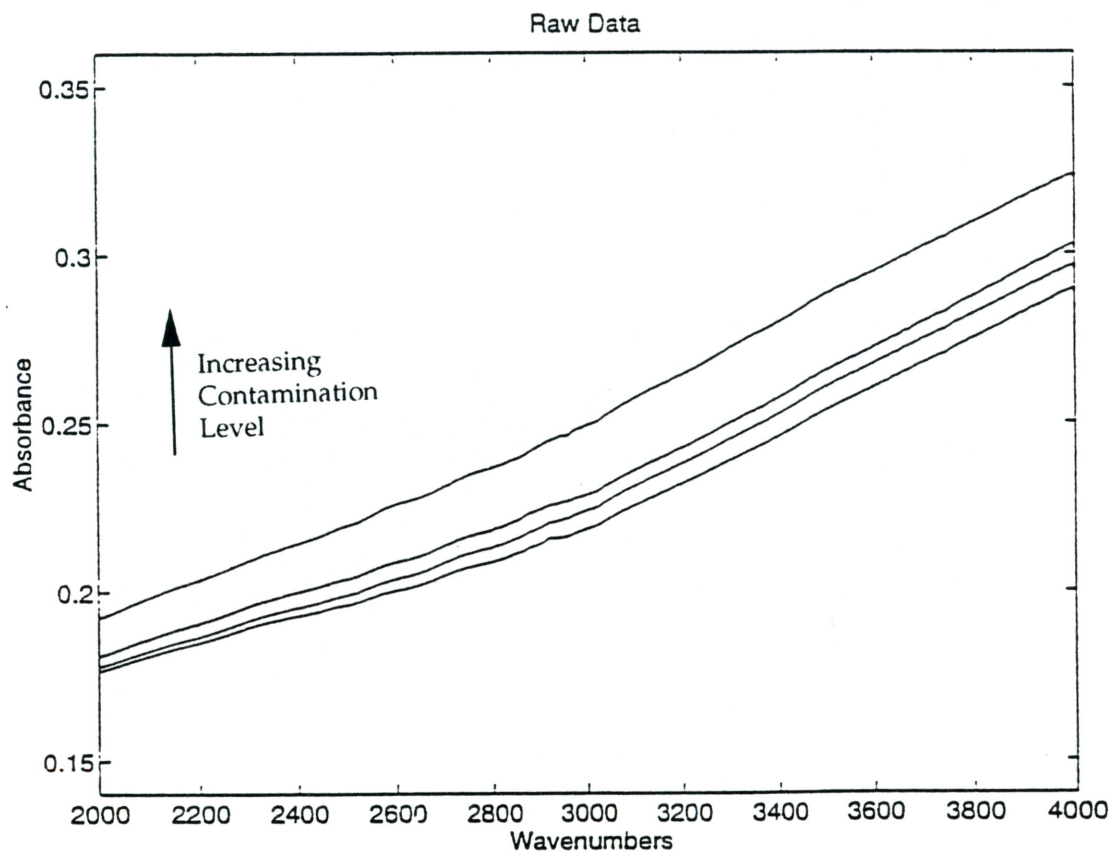


Figure 5.7 Overlaid raw infrared data for absorbance of oil on four cleaned metal coupons.



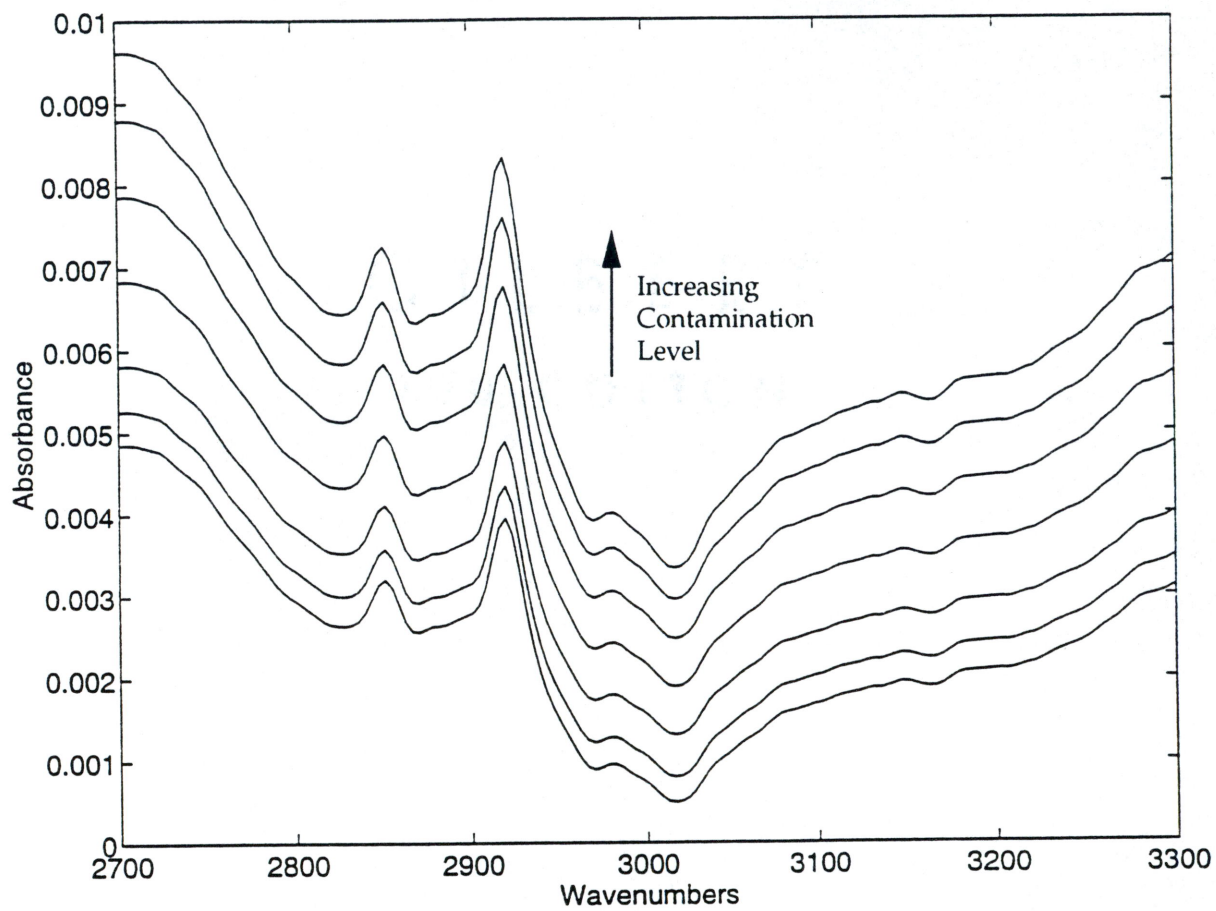


Figure 5.8 Overlaid infrared spectra showing increasing levels of oil contamination present on cleaned metal coupons.

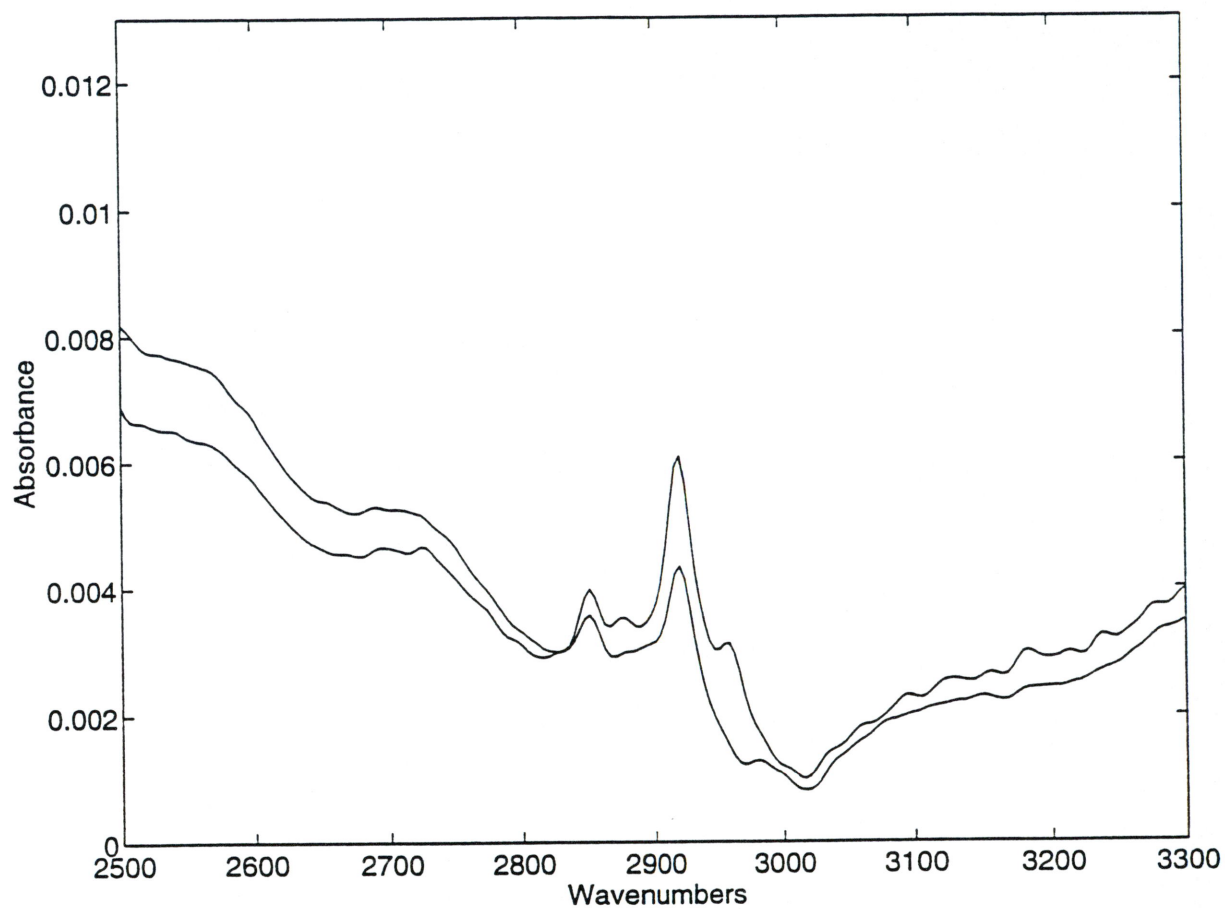


Figure 5.9 Overlaid infrared absorbance spectra for identical oil in approximately similar amounts on two different steel coupons.

### 5.3 Results from ultraviolet Fiber-Optic Spectrometry

The in-house ultraviolet instrumentation was tested to find its utility as a tool for detecting contamination on metallic surfaces. For most of the tests, stainless steel coupons (Part MC4) cleaned in the manner described in section 4.1, were used as samples. These parts were chosen because they fit the geometry requirements of having a small flat surface, the requirement of being an actual industrial part, and were made available in sufficient number for a variety of tests.

The first objective was to check in a consistent manner for instrument response to different contaminants on the surface. A reference measurement was made against a clean metal background, after which the metal was evenly contaminated. The surface was then tested for ultraviolet response at a few different spots, and over a small time interval, depending on the volatility of the contaminant.

Figure 5.10 shows the spectra for part MC4 coated with different degrees of a contaminant consisting of cutting fluid and various other oils. Seven spectra are shown, each corresponding to a different contamination level on the surface. Seven spectra were taken at each contamination level, and then averaged to obtain the resulting spectrum for that level. The several spectra taken at a single contamination level are shown in Figure 5.11. It can be seen from this figure that there is a high degree of consistency in the data. Since it is not possible to obtain the exact same level of contamination on a surface either by smearing or cleaning, this data was taken at different spots close to each other, in the shortest time

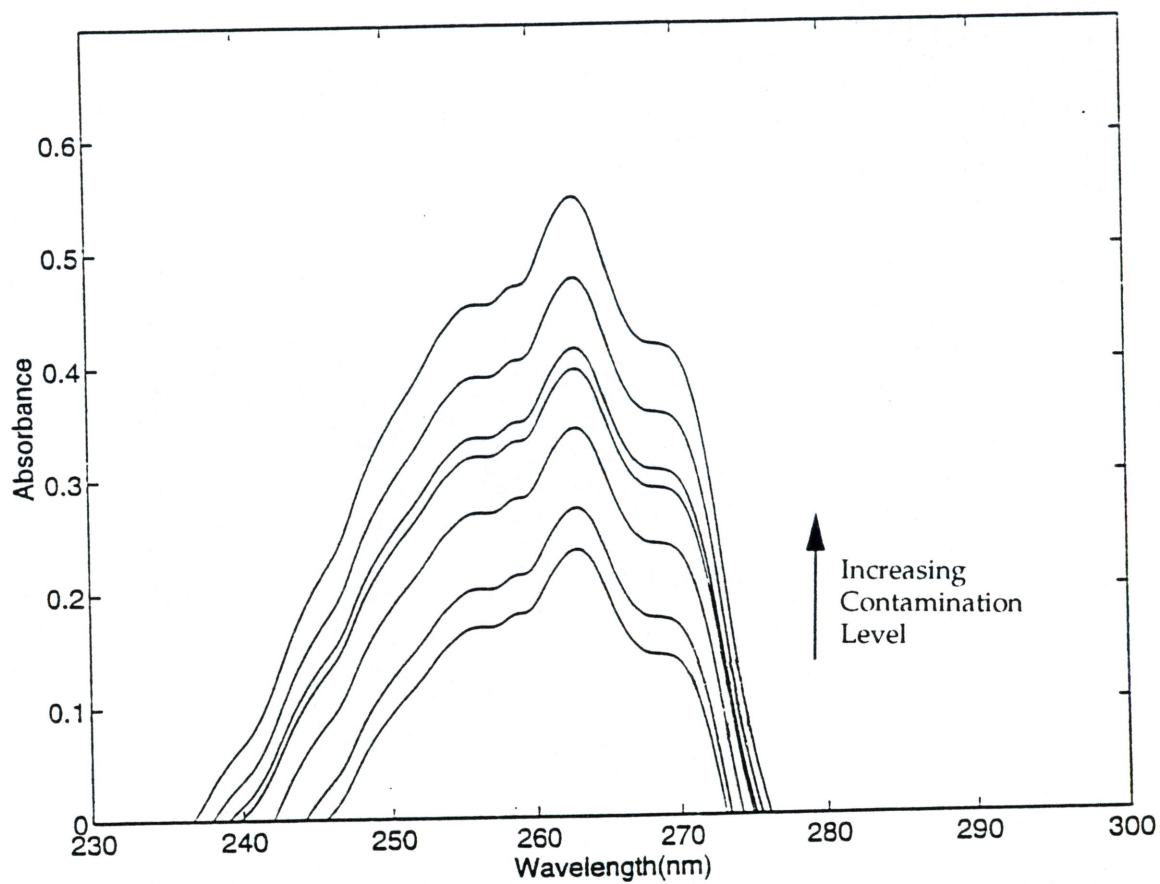


Figure 5.10 Overlaid ultraviolet absorbance spectra for metal part soiled with cutting fluids in the contamination range of 2 to 7 mg./square ft.



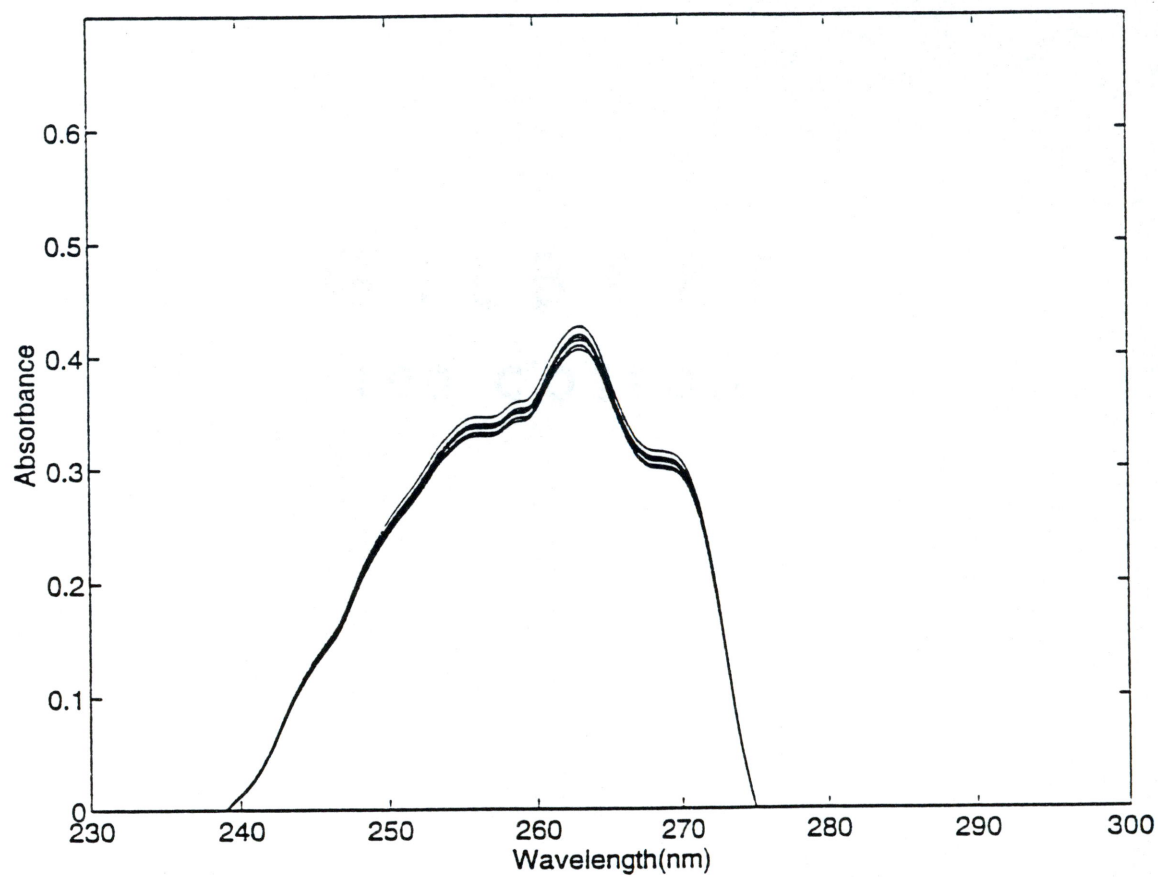


Figure 5.11 Seven overlaid ultraviolet spectra taken at the same contamination level.

span possible. Figure 5.12 shows the spectra for different levels of a power cutting fluid smeared on the part.

Parts cleaned with various cleaners were also analyzed to determine the amount of remaining residue from the contaminant, and the cleaner if any. It was seen that the results were consistent up to a certain low level of cleanliness. As the parts became cleaner, they approached the level of cleanliness of the reference sample, and hence very little signal was detected from the surface. A reading essentially consisting of noise was obtained in these cases. However, parts corresponding to these levels of cleanliness yielded good data when analyzed using ESCA. This shows that the ultraviolet technique is not as sensitive.

#### **5.4 Results from Gravimetric Testing**

Gravimetric testing is a simple, if time-consuming method for testing the cleanliness of metal parts. Parts of different geometries were tested when dirty and after the cleaning process. The amount of NVR and particulates was determined, and added to give the total contamination. This was divided by the surface area of the part to get the result in units of milligrams per square foot. Since the parts tested were of fairly simple geometry, a reasonably accurate estimate of the surface area was obtained from measurements made using a scale.

Truck skin segments contaminated with forming oils, huck oil, adhesives, and sealants, were cleaned and tested. The six available chemistries were used, along with three solvents provided by the company (TCA, Y1 and Y2). An experimental solvent (DUO) was also used. Wiping

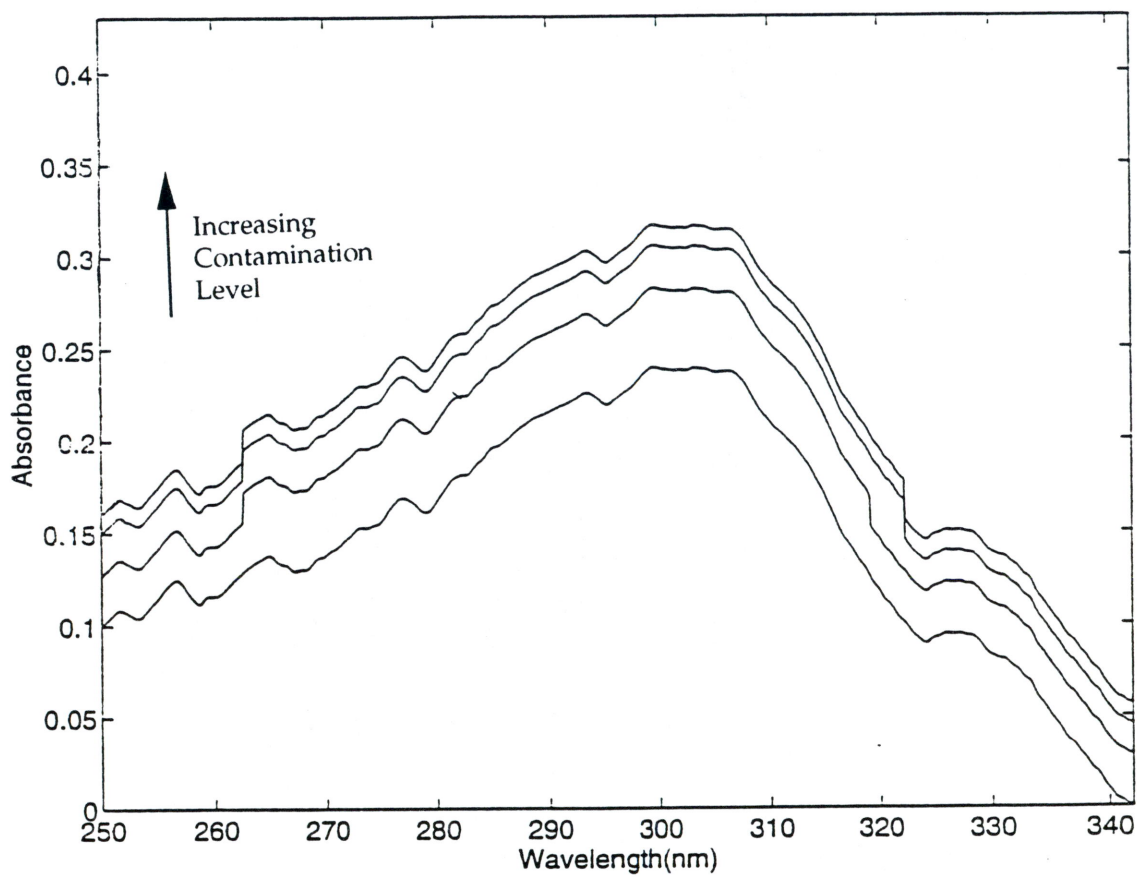


Figure 5.12 Four overlaid ultraviolet spectra for increasing levels of power cutting fluid on steel coupons.

was done at room temperature in a consistent manner using tissue paper. The panels were wiped with solvent, and allowed to dry. Table 5.2 shows the amount of contamination on parts before and after the wiping process.

Table 5.2 Results from gravimetric analysis of truck skin part coupons

Solvent Code	Particulates (mg/sq. ft.)	NVR (mg/sq. ft.)	Total Residue (mg/sq. ft.)
Dirty part	210.61	13.11	223.72
DUO	18.75	65.79	84.54
TE	11.31	10.03	21.34
AL	10.4	10.15	20.55
DBE	9.57	10.93	20.5
HC	8.75	10.83	19.58
RT	6.95	11.95	18.6
Y1	12.91	4.11	17.02
Y2	10.01	5.62	15.63
LPH	8.03	6.29	14.32
NMP	9.07	4.54	13.61
TCA	8.68	4.75	13.43
AC	9.35	0.83	10.18



## **5.5 Correlation of Results from Various Testing Methods**

Once consistent data was obtained from the four different cleanliness testing methods, an attempt was made to quantify and compare results from each of the methods. For this purpose, it was decided to convert all results into units of milligrams of contamination per square foot, since these are the units used in MIL-STD-1246B [1], which is treated as a standard by most industries and regulatory institutions. Besides quantification, correlation of the methods was another objective. To this end, results from all tests were compared in identical units.

### **5.5.1 Infrared vs. Ultraviolet**

A calibration plot for height of principle infrared peak vs. the amount of contamination in mg. per square foot, was generated. For each point, the sample was weighed thrice separately, and the results averaged in case the values were distinct from each other. A total of seven samples were used in the preparation of this plot. Each sample represented one level of contamination, and was scanned seven times, giving a total of 49 sample spectra.

### **IR Model**

The weight measurements were taken as the Y-data, and the matrix of spectra was taken as the X-block. In the preparation of a calibration model one must attempt to make sure that random noise or bad data does

not become part of the model, while at the same time trying to include all of the relevant spectral information available. A calibration model was made for the above data set using PLS and PCR and the results tabulated in Table 5.3. It was found that for both for PLS, the first factor accounted for slightly more information than for PCR. The second factor, while negligible, accounted for approximately the same amount of information using both methods. The contributions from other factors were even further smaller and attributed to random noise. Due to the higher amount of information contained in the first two PLS factors, this method was used to prepare the calibration.

Table 5.3 PCR vs. PLS, variance captured for IR model

5.3 (a) PCR		
Factor	X-Data % Variance	Y-Data % Variance
1	99.66	99.64
2	99.80	99.76
3	99.89	99.82
4	99.90	99.86
5	99.91	99.89
5.3 (b) PLS		
	X-Data % Variance	Y-Data % Variance
1	99.66	99.65
2	99.84	99.78
3	99.90	99.84
4	99.92	99.88
5	99.93	99.90

Cross validation was first performed by the leave-one-out method wherein a sample is left out and a model built with the rest of the samples.

This is done recursively until all samples have been left out once. A plot of the SEP(cv) versus the number of factors shows that the SEP(cv) values increases as the number of factors in the model is increased. This would suggest that a one-factor model would be optimal.

Cross validation was also done using the leave-a-group out technique whereby a group of samples is left out and a model is built with the remaining groups. The SEC and SEP values for this method, at each concentration level, are shown in Table 5.4. The SEC values decrease as more factors are added because more sample information is being added to the model. Too many factors must not be included in the final model since this can cause extraneous noise to creep in, which might not be representative. The determination of optimum number of factors is determined in great measure by the SEP values obtained from predicting data unknown to the model.

Table 5.4 SEC and SEP for leave-a-group-out validation

5.4 (a) SEC				
Level	Factors			
	1	2	3	4
1	1.21	1.08	0.91	0.79
2	1.49	1.12	0.98	0.88
3	1.53	1.16	1.02	0.91
4	1.57	1.17	1.04	0.94
5	1.53	1.14	0.99	0.86
6	1.55	1.16	1.04	0.93
7	1.49	1.11	0.96	0.83

5.4 (b) SEP				
Level	Factors			
	1	2	3	4
1	1.19	1.01	1.00	1.13
2	0.57	0.40	0.41	0.47
3	0.64	0.49	0.52	0.55
4	1.31	1.18	1.17	1.21
5	1.08	0.91	0.94	1.02
6	0.89	0.71	0.76	0.82
7	0.77	0.62	0.60	0.69

It is seen that the SEP values in this case do not follow a definite pattern. Inclusion of a second factor in the model does not seem to have a uniformly positive effect. The final infrared model was made after discard sets with the highest and the lowest SEP values. The SEC values showed an expected decrease with inclusion of factors, and the SEP values showed an increasing trend after one factor. Thus, a PLS model using one factor is proposed. The SEP and SEC values are plotted in Figure 5.13 and tabulated in Table 5.5. There is good agreement between the two real and predicted values.



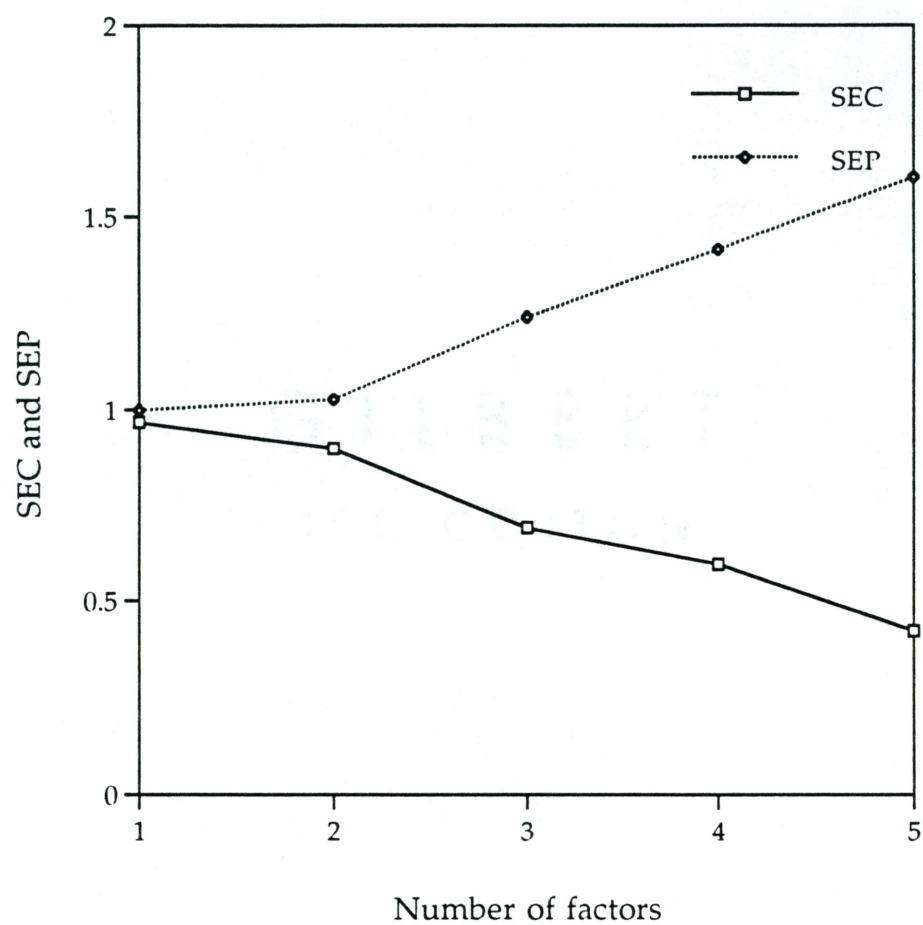


Figure 5.13. SEC and SEP vs. number of factors for PLS cross validation of infrared data.

Table 5.5 SEC and SEP values for IR model

Factors	SEC	SEP
1	0.99	1.00
2	0.90	1.02
3	0.69	1.24
4	0.58	1.41
5	0.42	1.61

### UV Model

The actual weight measurements were taken as the Y-data, and the matrix of spectra was taken as the X-block. In the preparation of a calibration model, one must attempt to make sure that random noise or bad data does not become part of the model, while at the same time trying to include all of the relevant spectral information available. A calibration model was made for the above data set using PLS and PCR. It was found that for PLS, the first two factors accounted for slightly more information than for PCR. The third factor, while negligible, accounted for approximately the same amount of information using both methods. The contributions from other factors are even further smaller, and attributed to random noise. The percent variance accounted for by the different factors using PCR and PLS is shown in Table 5.6. Due to the higher amount of information contained in the first two PLS factors, this method was used to prepare the calibration.

Table 5.6 PCR vs. PLS, variance captured

5.6 (a) PCR		
Factor	X-Data % Variance	Y-Data % Variance
1	97.88	97.63
2	99.79	99.40
3	99.85	99.51
4	99.89	99.75
5	99.91	99.78
6	99.92	99.80
5.6 (b) PLS		
	X-Data % Variance	Y-Data % Variance
1	98.22	98.04
2	99.87	99.85
3	99.90	99.88
4	99.91	99.90
5	99.93	99.91
6	99.93	99.92

The scores plot (Figure 5.14) for the first factor shows an increasing trend with increasing level of contamination. The second factor does not show a directional trend, but its not entirely insignificant contribution shows that there is unknown spectral information not accounted for by the first factor. The rest of the scores show little significance.

The spectra used in the PLS analysis were mean-centered and normalized. The second factor is shown to account for some relevant information. The contaminant oil was taken to contain a constant composition of its fixed different constituents. The second factor variations show that this might not be entirely true, and that there maybe extraneous material present in some cases. This could easily be explained

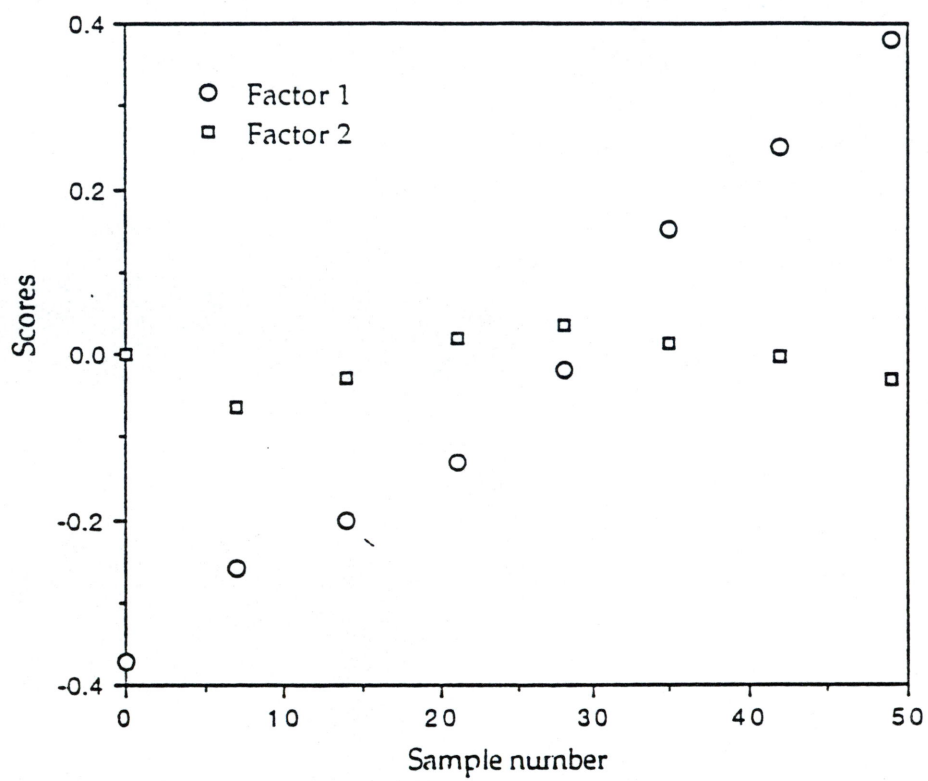


Figure 5.14 Scores plot for first two factors for ultraviolet data



in real terms by the possibility of minute contamination during manual handling of the parts. The third loadings for the other factors do not show a generally significant trend, and any variations can be attributed to local disturbances.

Validation of the model is necessary in order to test the accuracy of the calibration model in terms of information retained. By testing the model, the number of factors that need to be kept in the model can be confirmed. The two-factor calibration model was tested by a separate test set. The spectra corresponding to the two levels in set C were added to the calibration set, and a new calibration set was prepared. The standard error of prediction was calculated for the first seven levels, for different number of factors. The SEP values show a somewhat increasing trend after three factors, suggesting that the model must have at most three factors. SEP values for two and three factor models are almost the same. The SEP values determine how many factors are indeed optimal. From the data a two factor model was found to be reasonably adequate.

Set D, consisting of data taken at extremely low levels of contamination (less than 1 milligram per square foot) was then added to the calibration set, and another model was developed. It was seen that the inclusion of this data set led to a large reduction in the amount of information carried in the first two factors. Only 76 percent of the variation was explained by the first factor. This can be attributed to the fact that the spectra in Set D have a high noise content, due the ultraviolet instrumentation not being sensitive enough to obtain an accurate reading.

To further test the stability of the two factor model, the samples in Set C were included in the calibration, and sets one and six were removed.

The improved results in this case led to the re-forming of the calibration based on the leave-a-group-out cross validation method. In this method, data at one concentration level is left out, and a new calibration model is prepared. This is done for each level, until every level is excluded once. The results for this in terms of SEC and SEP for different number of factors included, is shown in Table 5.7. SEP values show a sharp decrease when the number of factors is increased from one to two. The trend from the second to the third factor is not clear, but the values are quite close to each other. Addition of the fourth factor leads to a sharp increase in SEP values, indicating that irrelevant data or noise is being included.

Leaving out sets two and four which had the highest and least SEP values, a new calibration model was prepared. It can be seen that the SEC values decrease with numbers of factors added, which is to be expected since more of the X-information is being included. This model shows an improvement in the SEP values for a two factor model (Table 5.8). This was taken to be the final model for the data set. Set D was excluded from these calculations. Using the final model, the predicted and actual levels of contamination were compared (Figure 5.15) and the SEP and SEC plots were made (Figure 5.16).

Table 5.7 SEC and SEP for leave-a-group-out validation

5.7 (a) SEC				
Level	Factors			
	1	2	3	4
1	1.21	1.08	0.91	0.78
2	1.49	1.12	0.98	0.88
3	1.53	1.16	1.02	0.90
4	1.57	1.17	1.04	0.93
5	1.53	1.14	0.99	0.87
6	1.55	1.15	1.04	0.93
7	1.48	1.11	0.96	0.83
5.7 (b) SEP				
Level	Factors			
	1	2	3	4
1	1.19	1.01	1.00	1.13
2	0.57	0.40	0.41	0.47
3	0.64	0.49	0.52	0.55
4	1.31	1.18	1.17	1.20
5	1.08	0.91	0.93	1.01
6	0.89	0.71	0.76	0.81
7	0.77	0.62	0.60	0.70

Table 5.8 SEC and SEP from final calibration model

5.8 (a) SEC				
Level	Factors			
	1	2	3	4
1	1.05	0.98	0.91	0.76
2	1.14	1.06	0.96	0.85
3	1.16	1.08	0.97	0.86
4	1.24	1.10	0.99	0.93
5	1.20	1.07	0.98	0.87
6	1.21	1.08	1.0	0.90
7	1.12	1.04	0.94	0.83
5.8 (b) SEP				
Level	Factors			
	1	2	3	4
1	1.08	0.99	0.96	1.0
2	0.54	0.39	0.40	0.44
3	0.58	0.42	0.43	0.47
4	1.11	1.03	1.03	1.10
5	1.03	0.90	0.90	0.97
6	0.86	0.70	0.71	0.77
7	0.77	0.62	0.60	0.68

### 5.5.2 Ultraviolet vs. Gravimetric

Ideally, the amount of weighed contamination from a simple weighing test before and after contamination should be the same as from weighing before and after cleaning the same sample. However, in reality, it is not possible to achieve the exact same level of cleanliness that existed prior to contamination and cleaning. Hence, the actual numbers from the gravimetric analysis of the test set are not the same as from the direct



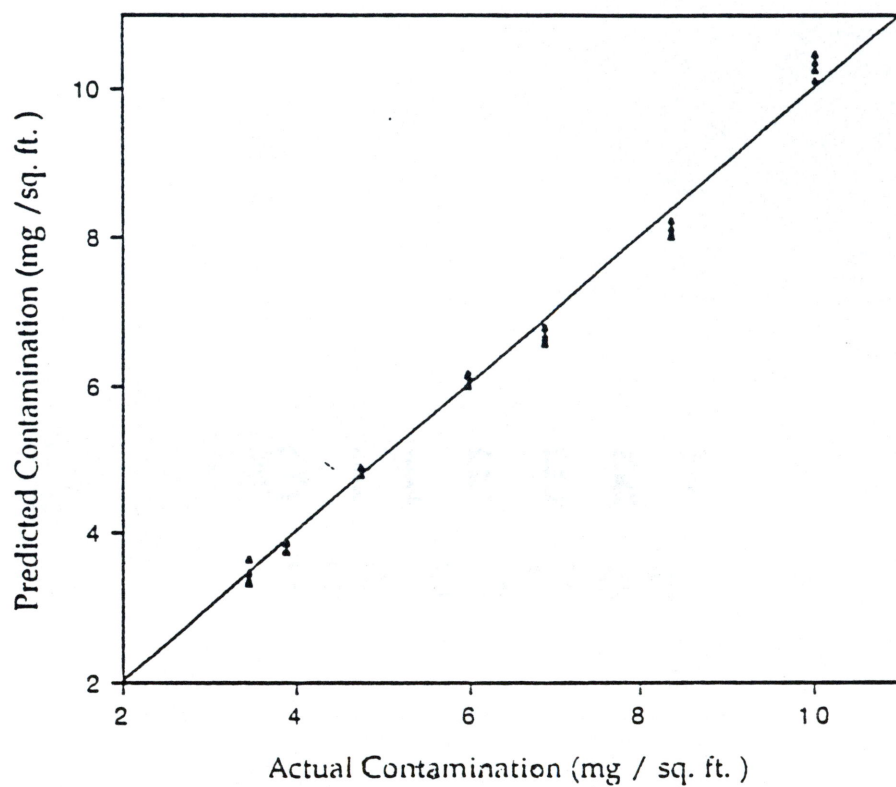


Figure 5.15 Scatter plot for predicted vs. actual contamination for PLS calibration model on ultraviolet data.

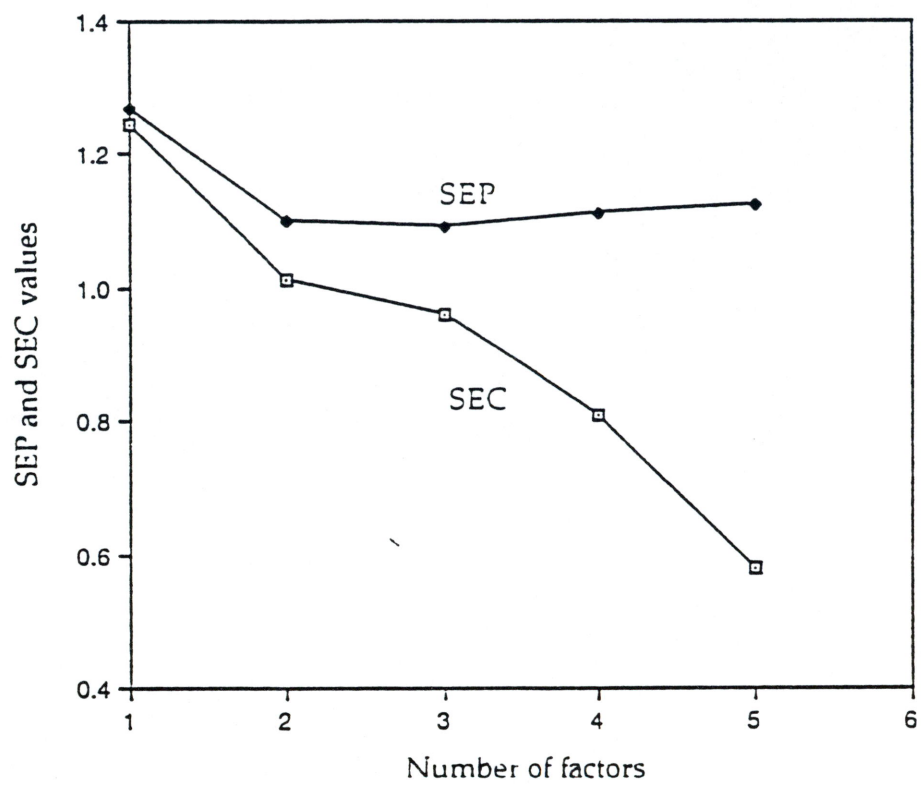


Figure 5.16 SEC and SEP plotted against number of factors for PLS cross validation on ultraviolet data.

weighing results. It can be expected though, that there will be some correspondence between the two sets of data.

The calibration model prepared in the earlier sections was used to predict concentrations of samples. Gravimetric testing was done on the same sample set, and the results were categorized as per the MIL-STD-1246B classification for NVR. The ultraviolet results were compared to the NVR testing based on the level of cleanliness achieved in both cases, and not the actual numerical quantities. The results are shown in Table 5.9.

Table 5.9 Comparison of cleanliness levels from model and gravimetric testing

Set	Prediction from model (level)	Gravimetric testing (level)	Contamination range (mg / square foot)
1	C	B	2 to 3
2	C	B	2 to 3
3	C	C	2 to 3
4	C	C	2 to 3
5	D	D	3 to 4
6	D	D	3 to 4
7	E	E	4 to 5
8	E	F	4 to 5
9	F	G	5 to 7

It can be seen from the above table that there is a fair degree of correspondence between the predicted results and the calculated level of cleanliness. The values for the gravimetric testing were all lower than the model predictions, possibly because of the difficulty in regaining all of the surface contamination through alcohol cleaning. In the case of spectroscopic measurements, it was possible to measure the parts at various spots to obtain a set of data at the same cleanliness level. The gravimetric method is, however, a one-shot measurement, and the results from such correlations will depend to a great extent on how much care is taken while doing the experiment. The repeated weighings and handling of sample cause this otherwise simple method to lose some of its accuracy. But the above results show that with careful sampling, it is possible to get a reasonably correct estimate of the cleanliness range of the part, if not a absolute and accurate measurement.

### 5.5.3 Ultraviolet vs. ESCA

As explained in Section 3.2.1, the determination of absolute concentrations on a surface using ESCA is a difficult proposition due to the knowledge of parameters required. The thickness of the contaminant layer and the density on the surface must be known in order to obtain weight information. ESCA results are hence represented as a ratio of peak areas or atomic percentages. In order to make some kind of a comparison between ESCA ratios and the results from ultraviolet spectrophotometry, a direct plot of atomic carbon-to-base metal ratio vs. predicted contamination was



made. The level of cleanliness from ESCA is determined by taking the carbon-to-base-metal ratio. While an actual weight measurement cannot be obtained with ease, it is possible to show that the trend in the predicted results matches the change in elemental compositions. The two methods are hence correlated in some manner.

#### 5.5.4 Comparison of Techniques

The predicted values of contamination were calculated using each of the four methods described above. Figures 5.17 to 5.20 show the relationship between actual weighed and model predicted values for each method. In order to show to the utility of the ultraviolet system, a comparative table showing the sum of squares of error against the respective cost, is presented in Table 5.10.

Table 5.10 Cost versus Prediction error for the four techniques

Method	Approx. Cost (Dollars)	Prediction Error
ESCA	700,000	1.39
Infrared	30,000	0.20
Ultraviolet	5,000	0.84
Gravimetric	800	2.54

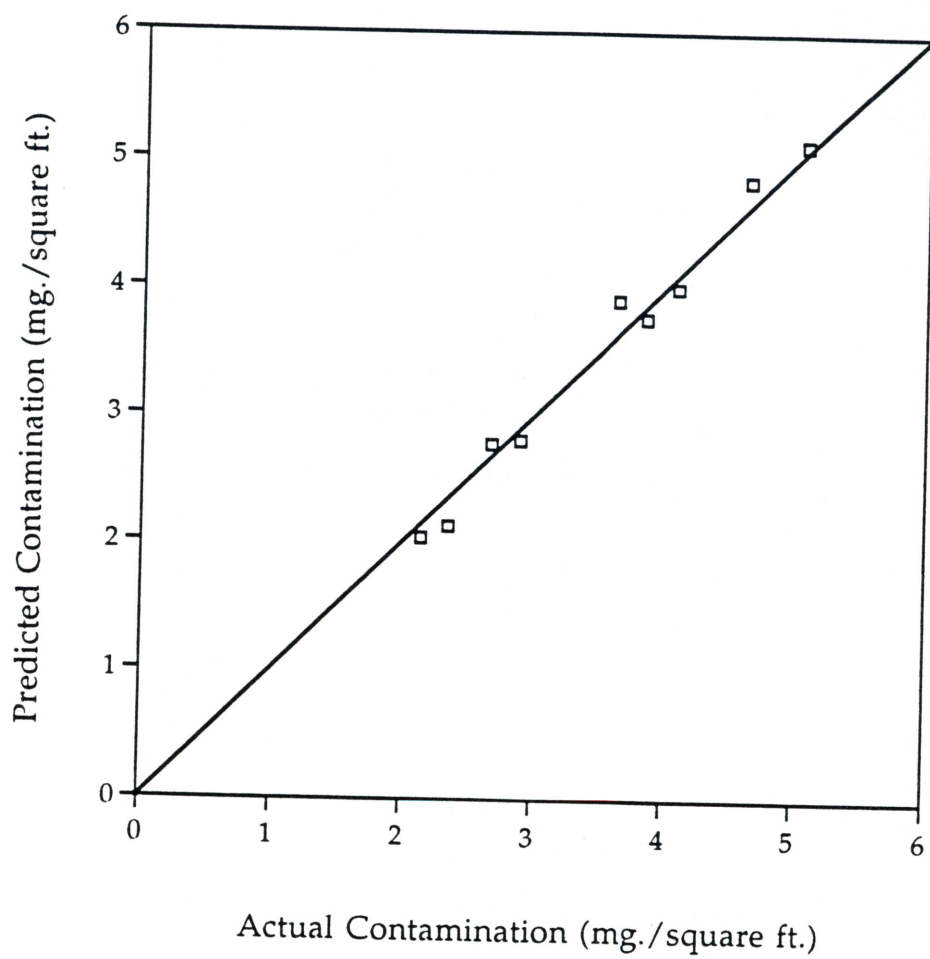


Figure 5.17 Predicted vs. Actual Contamination for Infrared

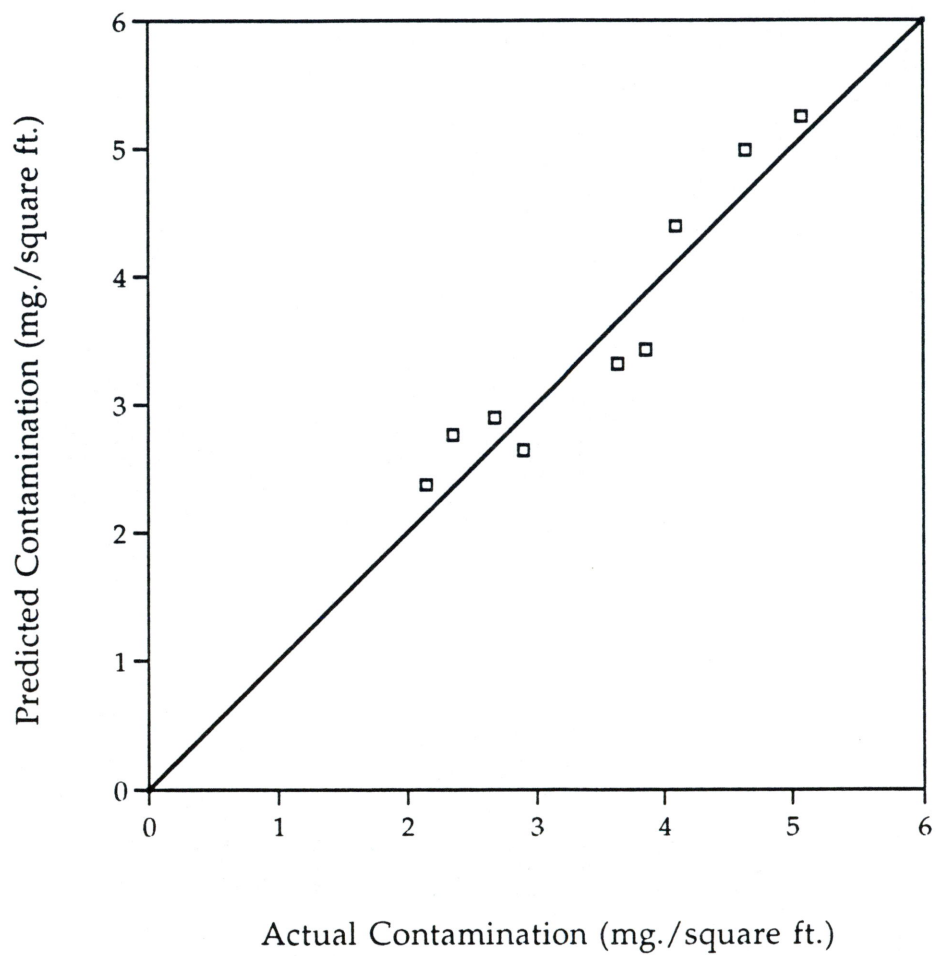


Figure 5.18 Predicted vs. actual contamination for ultraviolet

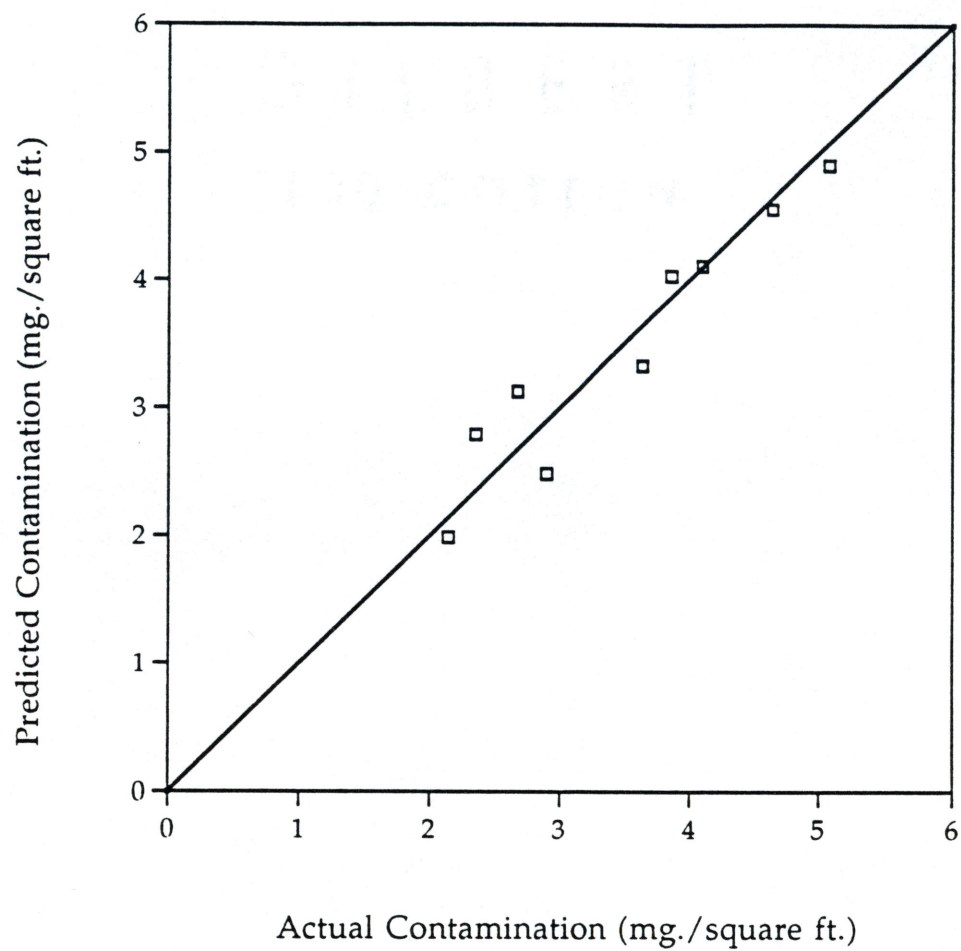


Figure 5.19 Predicted vs. Actual Contamination for ESCA



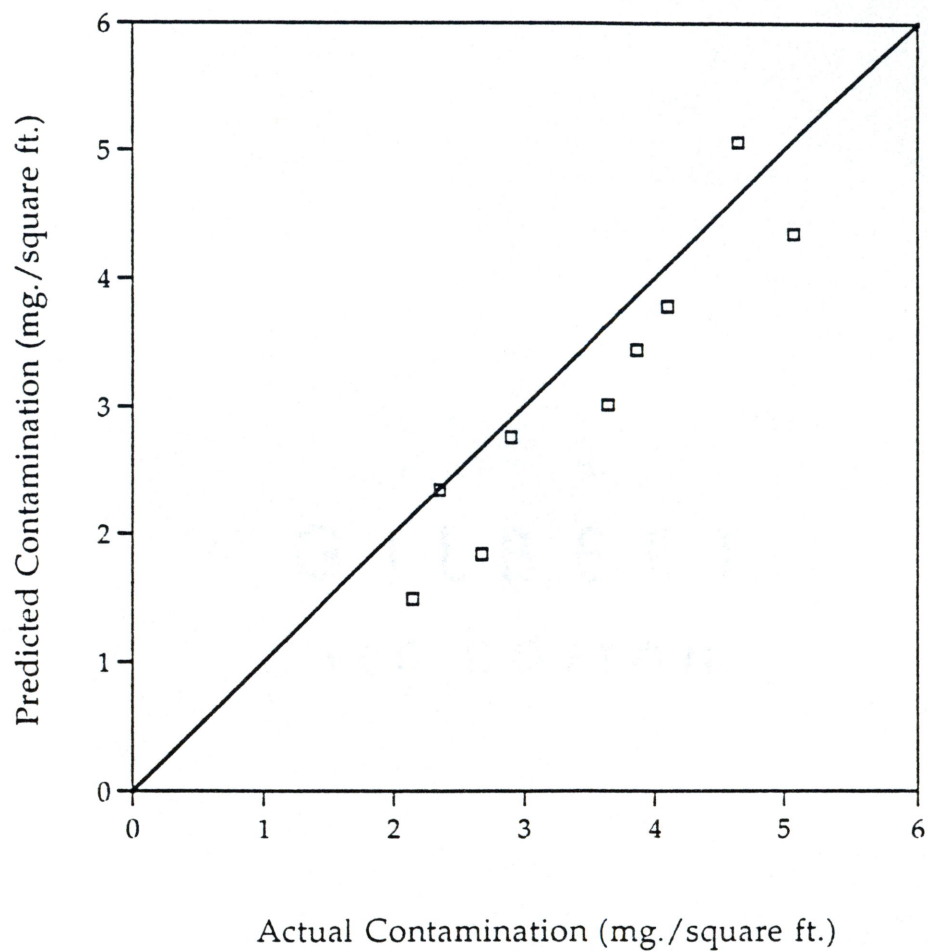


Figure 5.20 Predicted vs. actual contamination for gravimetry

Table 5.10 shows that while the ESCA instrument is expensive, its predictive ability is not very good. It must be noted here that since a direct conversion to appropriate units is not possible with ESCA data, predicted data was generated by plotting the carbon-to-metal ratios against the real data, drawing a calibration curve and replotting the data in appropriate units. The ESCA instrumentation was able to detect contamination corresponding to level B and lower (less than 2 mg. /square ft.) according to the military specifications. This method was found to be the most sensitive of the four techniques investigated.

The infrared method was determined to be the best as far as prediction was concerned. In the quantitative analysis for the infrared data, the minimum SEP was obtained by taking only one factor in the model. Hence this was used for building the final calibration model. The one-factor PLS model used predicted actual contamination levels with a standard error of prediction of 0.20. This accounted for 98.04 % of the variance in the Y-block data.

For the UV data, the SEP was found to be least for a two-factor model and hence two factors were used for building the calibration model. The ultraviolet technique compares favorably with infrared, given the fact that it costs only a sixth as much. The error from the UV method was four times that for the IR; however the predictions for the samples were still reasonably accurate.

The gravimetric method is inexpensive; however the predicted error is more than 10 times that for infrared. The predicted values from this method were consistently lower than the actual values. Since the

prediction errors are very large, this method is not suitable for detecting minor changes in contamination.

## 6. CONCLUSIONS AND FUTURE WORK

### 6.1 Conclusions

In this thesis, different methods of testing for the cleanliness of metal surfaces were discussed and the general utility of each method along with its advantages and disadvantages were pointed out. The SD-1000 ultraviolet fiber optic instrumentation was found to be an effective means for detecting organic contamination on the surfaces of metal parts.

Ultraviolet fiber optic spectrophotometry as described in this thesis has the advantages of quick data collection and portability. It was found to be consistently responsive to a given level of contamination. In addition, this method was shown to yield data comparable to spectroscopic tests which are far more expensive and time consuming.

Prediction of surface contamination levels was done using X-ray, infrared, ultraviolet, and gravimetric methods. All results were compared to contaminant weight data, and the error of prediction was calculated. From the results it was seen that a one-factor infrared model gave the most accurate results. Ranked next in accuracy, ultraviolet spectroscopy and ESCA yielded comparable results after conversion of the ESCA data to appropriate units; a two-factor ultraviolet model was used for making predictions on surface cleanliness. PCR and PLS gave corresponding results, with the PLS results being slightly better for the same number of factors. Gravimetric results were found to be the least accurate.

The four methods of testing were correlated by comparing each against data on the actual weight of contamination on soiled and cleaned



parts. A comparative look at the cost of each method and its accuracy showed that ultraviolet spectroscopy can be a very cost-effective testing method for the right kind of contaminants. Results generated from these tests were fed back to the partner companies to enable them to switch over to a more benign process and chemistry. It is expected that the companies will test the suitability of the parts cleaned via the new processes in the next stage of processing and pass the information to researchers, so that an attempt can be made to relate the degree of cleanliness to serviceability.

## 6.2 Future Work

The research done for this thesis indicated the directions that can be taken in surface cleanliness testing. As mentioned above, an attempt can be made to verify if cleaned parts actually perform adequately in the next process stage. If parts cleaned by a certain cleaner at a certain condition are found to match performance requirements, the cleaning conditions and amount of solvent used could be varied. Experiments can be conducted to determine the minimum level of cleanliness at which a part can be considered operational. This will require considerable experimentation and constant cross-checking to see if the part works in the process stage.

The fiber optic UV spectrometer can be made a powerful tool of analysis for the right kind of contaminants. If the contaminants are aromatic in nature and the company in question encounters few varieties of contamination, parts cleanliness determinations can conceivably be determined quickly by minimally trained personnel. Contamination profiles would have to be prepared for each manufacturer's contaminant, and a model developed based on that. Once a robust model is available, a

computer program can be written so that the amount of surface contamination is revealed in grams per unit area when the UV probe is shined onto the sample. A general database, consisting of calibration models for a general set of common substrates and contaminants encountered can be prepared from research such as described in this thesis.

The research indicates improvements to be made to UV measurement instrumentation. The two lowest contamination levels according to MIL-STD-1246B, did not yield satisfactory spectra and much noise was present. Increased detector sensitivity, better reference preparation and a holder for immobilizing the probe can be developed to enhance results from the UV instrument.

## **BIBLIOGRAPHY**

## BIBLIOGRAPHY

1. Guide to Cleaner Technologies: Alternatives to Chlorinated Solvents for Cleaning and Degreasing , *United States Environmental Protection Agency* (1991)
2. *From Pollution to Prevention* , U.S. Congress, Office of Technology Assessment, Washington, D.C. (September 1986)
3. T. Morehouse, "Update on the Montreal Protocol and the Air Force Pollution Prevention Program", *United States Environmental Protection Agency* (1993)
4. Executive Summary : Scientific Assessment of Stratospheric Ozone (1991)
5. Stratospheric Ozone Protection, Final Rule Summary, *United States Environmental Protection Agency* (March 1993)
6. Eliminating CFC-113 and Methyl Chloroform in Precision Cleaning Operations, *United States Environmental Protection Agency* (1991)
6. Guide to Cleaner Technologies : Alternatives to Chlorinated Solvents for Cleaning and Degreasing, *United States Environmental Protection Agency* (February 1994)
7. B. Carter, "Solvents-The Alternatives", *Waste Reduction Resource Center for the Southeast* (1993)
8. J. Matthews and K. Seuffer, "Development of Closed-Loop Chemistry/Water Recycling for Aqueous and Semi-Aqueous Formulations", *Waste Manage.* , Vol. 12, 1, 75 (1992)
9. C. D. D'Ruiz, *Aqueous Cleaning as an Alternative to CFC and Chlorinated Solvent-Based Cleaning* , Noyes Publications, New Jersey (1991)
10. B. Carlin, *Ultrasonics*, Mc-Graw Hill (1960)
11. R. T. Knapp, *Cavitation*, Mc-Graw Hill (1970)
12. G. L. Gooberman, *Ultrasonics : Theory and Application*, English Universities Press (1968)



13. B. A. Agranat *et al.*, "Ultrasonic Cleaning", in *Physical Principles of Ultrasonic Technology*, ed. L. D. Rosenberg, vol. I, Plenum Press, New York (1973)
14. D. H. McQueen, "Frequency Dependence of Ultrasonic Cleaning", *Ultrasonics* , **24**, 49-52 (1986)
15. V. A. Nosov, "Ultrasonics in the Chemical Industry", from *Soviet Progress in Applied Ultrasonics, Volume 2*, Consultants Bureau, New York (1965)
16. F. J. Fuchs, "The Role of Ultrasonics in Aqueous Cleaning", Paper presented at the *Parts Cleaning Technology Clinic* , Nashville (1993)
17. T. A. Carlson, *Photoelectron and Auger Spectroscopy* , Plenum Press (1975)
18. J. H. D. Eland, *Photoelectron Spectroscopy* , Wiley-Halsted, New York (1974)
19. P. K. Ghosh, "Chemical Analysis", in *Introduction to Photoelectron Spectroscopy* , Wiley-Interscience, New York (1983)
20. E. H. Baughman and D. Mayes, *Am. Lab* , Oct., 54 (1989)
21. H. H. Jaffe and M. Orchin, *Theory and Applications of Ultraviolet Spectroscopy* , John Wiley, New York (1964)
22. R. A. Friedel and M. Orchin, *Ultraviolet Spectra of Aromatic Compounds* , John Wiley, New York (1951)
23. M. G. Mellon, *Analytical Absorption Spectroscopy* , John Wiley (1970)
24. A. C. Hardy and F. M. Young, "The Correction of Slit-Width errors", *J. Opt. Soc. Am.* , **39**, 265 (1949)
25. G. Svehla, *Comprehensive Analytical Chemistry* , vol. IV, Elsevier, New York (1975)
26. P. Kubelka and I. Munk, *Z. Tech. Phys.* , **12**, 593 (1931)
27. H. Martens and T. Naes, *Multivariate Calibration* , Wiley, New York (1989)

28. B. R. Kowalski and M. B. Seasholtz, *J. Chemometrics*, **5**, 129 (1991)
29. P. Green, *Mathematical Tools for Applied Multivariate Analysis*, Academic Press, San Diego (1978)
30. D. M. Halland and E. V. Thomas, *Anal. Chem.*, **60**, 1193 (1988)
31. H. Wold, in *Multivariate Analysis*, ed. P. R. Krishnaiah, Academic Press, New York, 391 (1966)
32. J. Mandel, *The Amer. Statistician*, **36**, 15 (1982)
33. P. M. Lang and J. H. Kalivas, *J. Chemometrics*, **7**, 1 (1993)
34. P. Geladi and B. R. Kowalski, *Analytica. Chim. Acta.*, **185**, 1 (1986)
35. S. De Jong, *Chemometrics and Intelligent Laboratory Systems*, **18**, 251 (1993)
36. T. W. Wang, M. Berry, J. Batra, P. Sarma, A. Khettry and M. G. Hansen, paper presented at *First International Chemometrics Internet Conference*, (August, 1994)
37. B. M. Wise, *PLS\_Toolbox for use with MATLAB*, Version 1.2, A public domain software available through Barry M. Wise, 1415 Wright Avenue, Richland, WA 99352
38. G. J. Hof, *Present Practices in the Verification of Cleanliness*, Sandia Corporation Technical Memorandum, 147 (1963)
39. W. A. Zisman, "Constitutional Effects on Adhesion and Abhesion", in *Adhesion and Cohesion*, Elsevier (1962)
40. L.C. Cohen, "How Clean is Your "Clean" Metal Surface?", *Plating and Surface Finishing*, 58 (November, 1987)
41. A. Bragard et al., "Evaluation of the Surface of Cold-Rolled Steel Sheets", presented at the *10th Biennial Congress IDDRG*, Warwick (April, 1978)
42. A. W. Czanderna, *Methods and Phenomena: Their Application in Science and Technology*, Vol. 1, Elsevier (1975)

43. P. J. Sabatini, *Reactivation of Chromated Conversion Coatings for Maximum Paint Adhesion* , U. S. Naval Air Engineering Center Report AML-2503 (1966)
44. Thompson et al. , "Alternatives to CFCs" , *Oak Ridge National Laboratories Publication* (1992)
45. B. N. Ellis, *Circuit World* , Vol. 16, 4 (1989)
46. D. Samsami, *Electronic Packaging and Production* , 62 (1991)
47. IPC TR-580, "Cleaning and Cleanliness Test Program: Phase I and II Results" (1990)
48. K. L. Mittal, *Surface Contamination* , Vol. 1, Plenum Press, New York (1979)
49. J. J. Bikerman, "A Method of Measuring Contact Angles", *Ind. and Engr. Chem.* , 13, 443 (1941)
50. W. P. Innes, "Metal Cleaning", *Metal Finishing Guidebook* , 1993
51. B. L. Riddle, E. R. Price and T. E. Kirk, "Determinatuion of Mechanical Lubricants in Petroleum-Based Aluminum Rolling Oils," *Lubr. Engr.* , 41, 146 (1985)
52. J. T. Tanacredi, "Petroleum Hydrocarbons from Effluents Detection in Marine Environment," *Jour. Water Poll. Control. Fed* , 49, 216 (1977)
53. D. G. Anderson, "Coatings," *Anal. Chem.* , Vol. 61, 12, 33 (June, 1989)
54. *Industrial Cleaning Manual* , National Association of Corrosion Engineers, Houston, TX (1982)
55. R. L. Miller, "Rapid Method for Determining the Degree of Cleanliness of Metal Surfaces," *Materials Protection and Performance* (1973)
56. R. Nagarajan, "Surface Properties and Cleanability: A Rational Correlation," *Jour. of the IES* , 26 (January 1993)
57. W. C. Jones, "Testing Surfaces for Cleanliness", *Testing and Controls* , 12 (October 1985)
58. I. Lundstrom, University of Linkoping, Private Communication (1979)



59. M. Andrade, *Plat. and Surf. Fin.* , 73, 11 (1986)
60. S. Spring, "Industrial Cleaning," Prism Press, Melbourne (1974)
61. S. Spring *et al.* , *Ind. Eng. Chem. Anal. Ed.* , 18, 201 (1946)
62. L. E. Cohen and J. A. Hook, *Auto Laundry News*, 26 (August 1980)
63. F. A. Bystry and L. S. Penn, *Surf. and Interface Anal.* , 5, 98 (1983)
64. W. Gillum and A. Jackson, "Replacement of Chlorinated Solvents for In-Line Pre-Plate Metal Cleaning With Environmentally Sound Alternatives", *Metal Finishing* , 13 (August, 1992)
65. J. M. Farella, G. E. Mitchell and L. A. Bonadies, "The Development of Analytical Techniques for Quantitatively Comparing the Performance of Alternative Metal Cleaning Products", paper presented at the *International Conference on CFC Alternatives* , Baltimore, MD (December 1991)
66. W. T. Leijon, "Methods of Measuring Surface Cleanliness of Cold Rolled Steel Sheet", *Scand. J. Metallurgy* , 9, 189 (1980)
67. A. Horsthemke and J. J. Schroeder, "The Wettability of Industrial Surfaces", *Chem. Eng. Fund.* , Vol. 2, 66 (1983)
68. G. L. Powell *et al.* , "The Spectropus System: Remote Sampling Accessories for Reflectance, Emission, and Transmission Analysis Using Fourier Transform Infrared Spectroscopy", *Applied Spectroscopy* , Vol. 46, No. 1 (1992)
69. G. L. Powell, " Surface Inspection Using FTIR Spectroscopy", *Technical Interchange Meeting on Surface Contamination Analysis* , NASA, Marshal Space Flight Center (October, 1993)
70. W. F. Richey *et al.* , "New Analyses for Residual Rosin on Cleaned Electronic Circuit Boards", presented at *NEPCON West 1985* , Anaheim, CA (February, 1985)
71. W. L. Archer, T. D. Cabelka and J. L. Nalazek, "Quantitative Determination of Rosin Residues on Cleaned Electronic Assemblies", presented at the *SMART III Conference and Exhibition* , New Orleans, LA (January, 1987)



72. "How Dirty is Clean? XPS Will Tell", *Laser Focus World* , 149 (January, 1991)
73. K. W. Nebesny and N. R. Armstrong, *J. Electron Spec. and Related Phenom.* , **37**, 355 (1986)
74. N. Turner, B. Dulap and R. Colton, "Surface Analysis: X-Ray Photoelectron Spectroscopy, Auger Electron Spectroscopy, and Secondary Ion Mass Spectrometry", *Analytical Chemistry*, Vol. 56, **5**, 373 (1975)
75. M. P. Seah and H. J. Mathieu, "Method to Determine the Analysis Area of X-Ray Photoelectron Spectrometers - Illustrated by a Perkin-Elmer PHI 550 ESCA/SAM", *Rev. Sci. Instrum.* , Vol 56. **5**, 703 (May, 1995)
76. C. D. Wagner, in *Quantitative Surface Analysis of Materials* , N. S. McIntyre Ed., ASTM, Philadelphia, PA, 31 (1978)
77. K. W. Nebesny, B. L. Maschoff and N. R. Armstrong, "Quantitative Auger and X-Ray Spectroscopies", *Analytical Chemistry* , Vol. 61, **7**, 469 (April, 1989)
78. C. J. Powell et al. , *J. Surf. Interface Anal.* , **9**, 79 (1986)
79. U. Ray, I. Artaki, R. Ellis Jr., G. S. Heyer, "Hybrid Assembly Cleaning with Non-Halogenated Solvents", paper presented at the 1991 *International Conference on CFC Alternatives* , Baltimore, MD (December 1991)
80. "Instrumental Methods of Determining Surface Cleanliness", *SAE Society of Automotive Engineers* (July, 1989)
81. R. R. Willey, *Appl. Spectrosc.* , **30**, 593 (1976)
82. P. R. Griffiths and M. P. Fuller, in *Mid-Infrared Spectrometry of Powdered Samples* , Heyden, London (1982)
83. K. Krishnan and J. R. Ferraro, in *Fourier Transform Infrared Spectroscopy*, Vol. 3, 149, Academic Press, New York (1982)
84. R. M. Gendreau et al. , *Environ. Sci. Technol.* , **14**, 8 (1980)
85. M. D. Erickson, *Appl. Spectrosc. Rev.* , **15**, 261 (1969)
86. D. B. Judd and Wyszecki, *Color in Business, Science and Industry* , Wiley, New York (1963)

87. M. Jacobs and J. Waldrat, presented at the *Digilab User's Conf.* , Cambridge, Massachusetts (1980)
88. R. W. Hannah and R. E. Anacreon, *Appl. Spectrosc.* , **37**, 75 (1983)
89. L. V. Azarraga and A. C. McCall, presented at the *Pittsburgh Conf. Anal. Chem. Appl. Spectrosc.* , 25th, Cleveland, Ohio (1974)
90. S. A. Francis and A. H. Ellison, *J. Opt. Soc. Am.* , **49**, 131 (1959)
91. P. E. Nordal and S. O. Kanstad, *Int. J. Quant. Chem. Suppl.* , **12**, 115 (1977)
92. G. L. Powell, "Surface Inspection Using FTIR Spectroscopy", presented at the *Technical Interchange Meeting on Surface Contamination Analysis* , NASA, Marshal Space Flight Center (1993)
93. R. G. Greenler, *J. Chem. Phys.* , **44**, 310 (1966)
94. G. Kortum, *Reflectance Spectroscopy* , Springer-Verlag, New York (1969)
95. J. B. Bates and G. E. Boyd, *Appl. Spectrosc.* , **27**, 204 (1973)
96. M. Handke et L. , *J. Mater. Sci.* , **15**, 1317 (1980)
97. A. Ishitani *et al.* , presented at the *Pittsburgh Conf. Anal. Chem. Appl. Spectrosc.* (1980)
98. D. L. Wooton and D. W. Hughes, "Application of Reflectance Infrared Spectroscopy to the Lubrication Industry", *Lubrication Eng.* (September, 1987)
99. G. L. Powell *et al.* , " The Use of Remote-Sensing FT-IR Spectroscopy to Inspect the Surfaces of Ordinary Materials", presented at *PITTCO '93*, Atlanta, GA (March, 1993)
100. M. J. Smith *et al.* , "A Study of Blended Gasolines using FT-Raman and FT-IR Spectroscopy", *Spectrochim. Acta.* (November, 1991)
101. D. M. Haaland and E. V. Thomas, *Anal. Chem.* , **60**, 1193 (1988)
102. S. M. Haugland, E. Bahar and A. H. Carrieri, "Identification of Contaminant Coatings Over Rough Surfaces Using Polarized Infrared Scattering", *Applied Optics* , Vol. 31, **19**, 3847 (1992)

103. J. W. Childers, R. Rohl and R. A. Palmer, "Direct Comparison of the Capabilities of Diffuse Reflectance Spectroscopies in the Ultraviolet, Visible, and Near-Infrared Regions", *Anal. Chem.* , Vol. 60, 20, 1143, (1988)
104. K. R. Januszkiewicz and H. H. Sulek, "UV-Fluorescence Spectroscopic Method for Monitoring Tramp Oil Contamination in Hot Rolling Emulsions", *Lubrication Eng.* , 448 (June, 1991)
105. E. B. Murphy, "Solvent Contamination Determined by UV Reflection", *Proc. Inst. Envi. Sci.* , 123 (1985)
106. T. D. Cabelka, W. L. Archer and J. A. Trombka, "Cleaning SMCs with Chlorinated Solvents", paper presented at NEPCON West '86 , Anaheim, CA (1986)
107. J. E. Cahill, *Fundamentals of UV/Visible Spectrophotometry* , Perkin Elmer Bulletin No. ADS-123
108. H. J. Weltman and S. P. Evanoff, "Replacement of Halogenated Solvent Degreasing with Regenerable Aqueous Cleaners", presented at the 46th *Purdue Industrial Waste Conference* (1992)
109. T. D. Murphy Jr., "Design and Analysis of Industrial Experiments", *Chem. Eng.* , 168 (June, 1977)
110. C. P. Stafford, "Metal Cleaning in the '90s: Parameter Optimization and SAGE Advice for Alternative Cleaning Agents", Master's Thesis, University of Tennessee (August, 1995)
111. *Solvent Alternatives Guide* , computer program developed by the Research Triangle Institute Center for Aerosol Technology, Research Triangle Park (1993)
112. L. E. Davis, J. F. Riggs and C. D. Wagner, *Handbook of X-Ray Photoelectric Spectroscopy* , Perkin-Elmer Corporation, Minnesota (1979)
113. K. A. Kosanovich and M. J. Piovosio, "Process Data Analysis Using Statistical Methods", *E. I. Du Pont De Nemours & Co. Publication* (1991)
114. "Product Cleanliness Levels and Contamination Control", *MIL-STD 1246 B , Revision B* , (September, 1987)



## VITA

Vivekanand Sistla was born in Vijayawada, India on May 21, 1970. He attended high school at St. Josephs College, Allahabad. He secured admission to the Osmania University College of Technology (OUCT), Hyderabad, by ranking in the top 1% in the entrance examination. He was an active member of the Indian Institute of Chemical Engineers while at OUCT. He was also president of the Quiz Club and captained the table tennis team at OUCT. He graduated from Osmania University with a Bachelor of Technology in Chemical Engineering in June 1992. He received the Master of Science degree in Chemical Engineering from the University of Tennessee in August 1995.